

**SOLUTIONS OF THE LANDAU PROBLEM  
AND SOME USES OF THE DENSITY  
FUNCTIONAL THEORY IN MATERIALS  
SCIENCE**

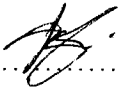
by  
**Elias Phiri**

THESIS  
MSC  
(PHYSICS)  
PHI  
2011  
C.1

**A dissertation submitted to the University of Zambia in partial  
fulfillment of the requirements for the degree of  
Master of Science in Physics**



I solemnly declare that this dissertation represents original work which has not been submitted for a degree at this or any other university.

Signature:  .....

Date: 27<sup>th</sup> July, 2011 .....

Name: ELIAS PHIRI .....

## Approval

This dissertation by Elias Phiri has been approved as fulfilling the requirements for the award of the degree of Master of Science in Physics by the University of Zambia.

Name:

Signature:

Date:

.....

.....

.....

External Examiner

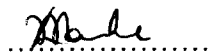
H.V. MWEENE.....



29/7/2011

Supervisor

m. lombe.....



02/08/2011

Internal Examiner

.....

.....

.....

Dissertation Chairperson

## **Dedication**

*This work is dedicated to my brother and sister, Mangiza and Chaona Phiri, with whom I share so many wonderful memories.*

## Abstract

The ordinary time-independent Landau problem of a charged particle moving in an external perpendicular homogeneous magnetic field and the case of when a linear potential is introduced are reviewed for motion occurring in an infinite plane, on an infinite strip and in the half-plane. The first objective of this part of the study is to obtain a semi-numerical solution of the modified Landau Hamiltonian for the case of motion in the half-plane; this is done using the discretization method. The structure of the energy eigenvalue spectrum is presented and an analysis of the results reveals that it is of the linear harmonic operator form with slight variations which are as a result of the addition of the linear perturbation. In an actual physical system such as a quantum Hall slab, the linear perturbation could be an electric field or a gravitational quantum well.

The second objective of this part of the study is to investigate Landau quantization in a two-dimensional electron gas by working in the Landau gauge. Such a system can actually be physically created at semiconductor heterojunctions. Our results reveal that the degree of degeneracy in the energy levels becomes finite if the motion is restricted to an area and the differential equation that governs this motion is the same as that presented in the first part of the study for the case of motion in the half-plane.

Within the Density Functional Theory (DFT), an introduction to the self consistent field method for solving the Kohn-Sham system is also presented. The objective of this part of the study is to investigate the stability and formation sequence of the NiGe, Ni<sub>2</sub>Ge, Ni<sub>3</sub>Ge<sub>2</sub> and Ni<sub>5</sub>Ge<sub>3</sub> thin film phases; this is accomplished by using an open-source computer program called QUANTUM ESPRESSO.

A comparison of our results with those obtained from experiments reported in the literature proves that significantly accurate predictions of the properties of materials can be made by using DFT methods.

Ultimately our results show that the Ni<sub>2</sub>Ge, Ni<sub>3</sub>Ge<sub>2</sub> and Ni<sub>5</sub>Ge<sub>3</sub> phases are more stable and hence must form in the first phase while NiGe is less stable and should form in the second phase.

## Acknowledgements

Firstly, I would like to thank my sponsors the SEM (Solar Energy Materials) Project of the University of Zambia in conjunction with Uppsala University for awarding me a scholarship to carry out this work.

I owe a lot to my two supervisors Dr A. Habanyama and Dr H. V. Mweene for being a great source of personal inspiration and offering me constant guidance and support during the course of my research work. Despite having heavy workloads, they both always managed to accommodate me whenever I sought their assistance.

I would like to thank my friends and fellow Master of Science students Mr. Moses Tembo and Mr. Joseph Simfukwe with whom I endured so much; crafting solutions to physics problems and studying. They offered me a lot of support and their general comments were of great help in seeing the completion of my work.

I am also indebted to many in the Department of Physics but I will limit myself to thanking those who I feel showed the most concern; Prof. Karouyero for his work as the Postgraduate committee chairperson, his timely interventions in all matters that had to do with the submission of my research proposal and dissertation made the rest of my work proceed smoothly, Dr Hatwaambo for facilitating my trip to France and ensuring that all the money matters were addressed whenever problems arose, and the three technicians Mr. Bundala, Chibwe and Changwe for their individual significant contributions that ultimately led to the completion of my work.

Finally, I would like to thank my entire family and close friends for their constant encouragement and support.

## Units

Almost all the equations used in this study are written in SI rationalized units. However, when referring to numerical values in the body of the text or in diagrams, whatever units that seem most appropriate to the quantity being described are used as is the case for the total ground state energies presented in the density functional theory calculation. They are quoted in Rydberg rather than electron volts.

# Table of Contents

<b>Declaration</b>	<b>ii</b>
<b>Approval</b>	<b>iii</b>
<b>Dedication</b>	<b>iv</b>
<b>Abstract</b>	<b>V</b>
<b>Acknowledgement</b>	<b>Vi</b>
<b>Units</b>	<b>vii</b>
<b>1. Introduction</b>	
<b>1.1 The Landau Problem and Density Functional Formalism</b>	<b>1</b>
<b>1.2 Charged Particles in Electromagnetic Fields</b>	<b>3</b>
<b>1.2.1 The Lagrangian and Hamiltonian of a Charged Particle</b>	<b>5</b>
<b>1.2.2 Gauge Invariance in the Schrödinger Equation</b>	<b>8</b>
<b>1.2.3 Gauge Invariance in Hamilton's Equation</b>	<b>11</b>
<b>1.2.4 Gauge Dependence of the Canonical Momentum</b>	<b>15</b>
<b>1.2.5 Gauge Fixing in Classical Gauge Theories</b>	<b>17</b>
<b>1.3 The Density Functional Theory</b>	<b>17</b>
<b>1.3.1 Physical picture - Hohenberg-Kohn Theorems</b>	<b>18</b>
<b>1.3.2 The Kohn-Sham Equations: Exchange and Correlation Effects</b>	<b>21</b>
<b>1.3.3 The Local Density Approximation</b>	<b>24</b>
<b>1.3.4 The Generalized Gradient Approximation</b>	<b>25</b>
<b>2. Algebraic Solution of the Landau Problem</b>	
<b>2.1 Introduction</b>	<b>26</b>
<b>2.2 The Ordinary Landau Problem</b>	<b>28</b>
<b>2.3 The Landau Problem with a Linear Potential</b>	<b>31</b>
<b>2.3.1 The Landau Problem in an Infinite-Plane with a Linear Potential</b>	<b>32</b>
<b>2.3.2 The Landau Problem in the Half-Plane with a Linear Potential</b>	<b>37</b>
<b>3. Computational Solution of the Landau Problem</b>	
<b>3.1 Introduction</b>	<b>42</b>
<b>3.2 Discretization Method</b>	<b>43</b>



3.2.1 The Finite Difference Method	43
3.2.1.1 The Taylor Series and Approximation of the First Derivative	44
3.2.1.2 Approximation of the Second Derivative	44
3.2.2 The Finite Difference Formulation and the Solution of the Landau Problem in the Half-plane with a Linear Potential	45
3.3 Landau Quantization in a Two-Dimensional Electron Gas	50
4. Some uses of Density Functional Theory in Materials Science	
4.1 Introduction	56
4.2 Plane Wave Self-Consistent Field (PWscf) Calculations	57
4.2.1 Self-Consistent Field Cycle	60
4.2.2 Density Functional Methods in the Study of Crystalline Materials	61
4.3 Results	62
4.3.1 Convergence for Plane-Wave Energy Cut-off	65
4.3.2 Convergence for K-Point Mesh Density	67
4.3.3 Calculation of the Lattice Parameter	69
4.4 Stability of Nickel Germanides	71
5. Discussion and Conclusion	
5.1 The Landau Problem	73
5.2 The Density Functional Theory and its Applications in Materials Science	75
Appendix	77
References	84

## 1.0 Introduction

---

### 1.1 The Landau Problem and Density Functional Formalism

The ordinary Landau problem is met with in various physical contexts [1] and involves the study of the dynamics of a charged particle in a homogeneous perpendicular magnetic field.

Over the years, many variations of the Landau problem have been presented and studied [1]. These mostly involve the introduction of other potentials for which exact solutions are rarely feasible [2].

In this chapter, the time-independent ordinary Landau problem as is encountered in classical electrodynamics is reviewed. Starting from a classical electrodynamics introduction, a quantum mechanical treatment is considered. The derivation of the Lagrangian and Hamiltonian of a charged particle in a homogeneous perpendicular magnetic field proceeds from the variational principle and finally leads to the Schrödinger equation for the system.

The property of gauge invariance in the Schrödinger equation derived from the Landau Hamiltonian is studied and for the Hamilton equations, their gauge invariance property is proved and the gauge dependence of the canonical momentum is studied.

Finally, some gauge fixing theories of classical electromagnetism are introduced and the most common non-relativistic as well as relativistic gauges are presented.

We present a general discussion of the concepts that govern the density functional theory (DFT) in this chapter.

The Hamiltonian used to model many body systems within DFT is an approximation, thus there are always errors in the results obtained from DFT calculations depending on the type of system

being studied. The errors in most of the calculations are known to stem from the approximation of the exchange correlation functional; thus, we conclude this introductory chapter by discussing the local density and generalized gradient approximations for the exchange correlation energy which have been known to produce good results for atoms and molecules.

In summary, no entirely new material is being introduced in this chapter. The objective is firstly to introduce the time-independent ordinary Landau problem; derive the key equations that govern motion of a charged particle in an electromagnetic field, thereby establishing a mathematical background which is critical for the analysis of variations of the time-independent Landau problem studied in the next two chapters and secondly, to introduce the Density Functional formalism; the Hohenberg-Kohn theorems, review of exchange-correlations effects and to introduce the popular approximation methods to the exchange-correlation functional that are used in the computer application used to perform DFT calculations in this study.

### 1.2 Charged particles in electromagnetic fields

It is well known from classical electromagnetism that when a particle of charge  $e$  moves with velocity  $\mathbf{v}$  in an electromagnetic field, it experiences the Lorentz force [1].

$$\mathbf{F} = e \left( \mathbf{E} + \frac{\mathbf{v}}{c} \times \mathbf{B} \right) \quad (1.2.0)$$

If the charged particle is of mass  $m$  and if the force (1.2.0) is the only force acting on it, then from Newton's second law, the equation of motion is derived as

$$m \frac{d\mathbf{v}}{dt} = e \left( \mathbf{E} + \frac{\mathbf{v}}{c} \times \mathbf{B} \right) \quad (1.2.1)$$

Since the force  $e(\mathbf{v}/c \times \mathbf{B})$  is perpendicular to the direction in which the particle is moving, the work done by the force is zero. Hence this force does not appear in the conservation of energy equation

$$\frac{1}{2}mv^2 - \int e\mathbf{E} \cdot d\mathbf{r} = \text{constant} \quad (1.2.2)$$

The electric and magnetic fields acting on the particle can be expressed by their corresponding potentials  $\mathbf{A}(\mathbf{r}, t)$  and  $\phi(\mathbf{r}, t)$ . If the potential energy due to the electric field is written as  $e\phi$ , the energy conservation equation (1.2.2) takes the form

$$\frac{1}{2}mv^2 + e\phi = \text{constant} \quad (1.2.3)$$

We now consider one of the simplest motions discussed in the literature [2]. The motion of a charged particle moving in an electromagnetic field characterized by  $\mathbf{E} = 0$  and  $\mathbf{B} = \text{constant}$ . If the  $z$ -axis is chosen to be parallel to  $\mathbf{B}$  so that  $\mathbf{B} = B\mathbf{k}$ , where  $B$  is constant, the equation of motion (1.2.1) can be written as

$$m \frac{d\mathbf{v}}{dt} = eB \frac{\mathbf{v}}{c} \times \mathbf{k} \quad (1.2.4)$$

The adoption of a Cartesian coordinate system and replacement of the velocity vector with the expression  $\mathbf{v} = \dot{x}\hat{i} + \dot{y}\hat{j} + \dot{z}\hat{k}$ , enables us to write the three components of the equation of motion as

$$m\ddot{x} = eB \frac{\dot{y}}{c} \quad (1.2.5a)$$

$$m\ddot{y} = -eB\frac{\dot{x}}{c} \quad (1.2.5b)$$

$$m\ddot{z} = 0 \quad (1.2.5c)$$

Eliminating  $\ddot{y}$  between equation (1.2.5b) and the derivative of equation (1.2.5a) gives

$$\ddot{x} + \omega^2 \dot{x} = 0, \quad \omega = e \frac{B}{mc} \quad (1.2.6)$$

This is the simple harmonic motion equation [3] for  $\dot{x}$ , and it has the solution

$$\dot{x} = R \sin(\omega t + \delta) \quad (1.2.7)$$

Substitution of the derivative of (1.2.7) into equation (1.2.5a) gives

$$\dot{y} = R \cos(\omega t + \delta) \quad (1.2.8)$$

Integration of (1.2.7) and (1.2.8) with respect to time yields

$$x = -\frac{R}{\omega} \cos(\omega t + \delta) + x_0, \quad y = \frac{R}{\omega} \sin(\omega t + \delta) + y_0 \quad (1.2.9)$$

where  $x_0$  and  $y_0$  are constants of integration. To eliminate the trigonometric functions, we add the squares of (1.2.9) and get

$$(x - x_0)^2 + (y - y_0)^2 = \frac{R^2}{\omega^2} \quad (1.2.10)$$

We observe that the motion of the particle in the  $xy$  plane describes a circle of radius  $R/\omega$  centered on the point  $(x_0, y_0)$ . Squaring and adding the equations (1.2.7) and (1.2.8) also gives

$$\dot{x}^2 + \dot{y}^2 = R^2 \quad (1.2.11)$$

This shows that the speed and angular velocity of the particle are  $R$  and  $\omega$  respectively.

According to equation (1.2.5c), the particle has a constant speed in the  $z$  direction so that the path of the particle is a helix, with the axis of the helix being parallel to the  $z$ -axis.

### 1.2.1 The Lagrangian and Hamiltonian of a Charged Particle

The effect of the electromagnetic field on a charged particle can be described by a velocity-dependent generalized potential [1]. From the Lorentz force, the generalized potential, the Lagrangian and the Hamiltonian can be derived. Classically, the total energy of the physical system is described by the Hamiltonian while in quantum mechanics, if the form of the Hamiltonian is known, the Schrödinger wave equation determines the wave functions and energy eigenvalues of the physical system concerned [4].

Consider the Lorentz force

$$\mathbf{F} = e \left( \mathbf{E} + \frac{\mathbf{v}}{c} \times \mathbf{B} \right) \quad (1.2.12)$$

where the electric and magnetic fields are expressed through potentials as

$$\mathbf{E} = -\nabla\phi - \frac{1}{c} \frac{\partial \mathbf{A}}{\partial t},$$

and

$$\mathbf{B} = \nabla \times \mathbf{A} \quad (1.2.13)$$

When we substitute equations (1.2.13) into the Lorentz force (1.2.0) we obtain

$$\mathbf{F} = e \left( -\nabla\phi - \frac{1}{c} \frac{\partial \mathbf{A}}{\partial t} + \frac{\mathbf{v}}{c} \times (\nabla \times \mathbf{A}) \right) \quad (1.2.14)$$

Use of the vector identity

$$\mathbf{B} \times (\nabla \times \mathbf{C}) = \nabla(\mathbf{B} \cdot \mathbf{C}) - (\mathbf{B} \cdot \nabla)\mathbf{C} - (\mathbf{C} \cdot \nabla)\mathbf{B} - \mathbf{C} \times (\nabla \times \mathbf{B}) \quad (1.2.15)$$

allows us to transform the triple vector product of (1.2.14) to

$$\mathbf{v} \times (\nabla \times \mathbf{A}) = \nabla(\mathbf{v} \cdot \mathbf{A}) - (\mathbf{v} \cdot \nabla)\mathbf{A} \quad (1.2.16)$$

The velocity  $\mathbf{v}$  is not an explicit function of the position thus we can write the total derivative of the vector potential with respect to time as

$$\frac{d\mathbf{A}}{dt} = \frac{\partial \mathbf{A}}{\partial t} + (\mathbf{v} \cdot \nabla)\mathbf{A} \quad (1.2.17)$$

Replacing the vector product of (1.2.14) by the relationships (1.2.16) and (1.2.17) gives the Lorentz force

$$\mathbf{F} = e \left[ -\nabla\phi + \frac{1}{c} \nabla(\mathbf{v} \cdot \mathbf{A}) - \frac{1}{c} \frac{d\mathbf{A}}{dt} \right] \quad (1.2.18)$$

Using Lagrangian formalism, we can deduce generalized forces  $Q_i$  from a velocity-dependent potential  $U(q_i, \dot{q}_i)$  [2]. The generalized forces are expressed by

$$Q_i = -\frac{\partial U}{\partial q_i} + \frac{d}{dt} \left( \frac{\partial U}{\partial \dot{q}_i} \right) \quad (1.2.19)$$

Assuming that  $\mathbf{A} = \mathbf{A}(p_i, q_i, t)$  then from the definition of the total temporal derivative of a function  $\mathbf{F}(p_i, q_i, t)$  in curvilinear coordinates [2], we can also define the total derivative of the vector potential as

$$\frac{d\mathbf{A}}{dt} = \frac{\partial \mathbf{A}}{\partial t} + \sum_{i=1}^f \left( \frac{\partial \mathbf{A}}{\partial q_i} \dot{q}_i + \frac{\partial \mathbf{A}}{\partial p_i} \dot{p}_i \right) \quad (1.2.20)$$

Here,  $p_i, q_i$  are the generalized momenta and coordinates, respectively,  $t$  is the time and  $f$  is the number of degrees of freedom. By considering a Cartesian coordinate system and substituting the corresponding expressions for the linear momentum,  $\mathbf{p} = m\mathbf{v}$  and coordinates, an expansion of equation (1.2.20) gives the total time derivative of the vector potential as

$$\frac{d\mathbf{A}}{dt} = \frac{\partial \mathbf{A}}{\partial t} + \nabla(\mathbf{A} \cdot \mathbf{v}) + \frac{d}{dt} \nabla_v(\mathbf{A} \cdot \mathbf{v}) \quad (1.2.21)$$

where  $\nabla_v$  signifies the derivative with respect to the three components of the velocity and we have also used  $\dot{\mathbf{p}} = m \frac{d\mathbf{v}}{dt}$ .

The velocity and vector potential can be written in their component forms as

$$\mathbf{v} = v_x \hat{i} + v_y \hat{j} + v_z \hat{k}$$

and

$$\mathbf{A} = A_x \hat{i} + A_y \hat{j} + A_z \hat{k} \quad (1.2.22)$$

Then  $\nabla_v(\mathbf{A} \cdot \mathbf{v})$  can also be written as

$$\begin{aligned} \nabla_v(\mathbf{A} \cdot \mathbf{v}) &= \left( \hat{i} \frac{\partial}{\partial v_x} + \hat{j} \frac{\partial}{\partial v_y} + \hat{k} \frac{\partial}{\partial v_z} \right) (A_x v_x + A_y v_y + A_z v_z) \\ &= (A_x \hat{i} + A_y \hat{j} + A_z \hat{k}) \end{aligned} \quad (1.2.23)$$

Thus the total time derivative of the vector potential can also be expressed as

$$\frac{d}{dt} \nabla_{\mathbf{v}}(\mathbf{A} \cdot \mathbf{v}) = \frac{d}{dt} (A_x \hat{i} + A_y \hat{j} + A_z \hat{k}) = \frac{d\mathbf{A}}{dt} \quad (1.2.24)$$

For a comparison with (1.2.19), we write

$$\frac{d\mathbf{A}}{dt} = \frac{d}{dt} \nabla_{\mathbf{v}}(\mathbf{A} \cdot \mathbf{v}) \quad (1.2.25)$$

Taking the  $x$  component and comparing it with (1.2.18) and (1.2.19) using the relation (1.2.25), we can express the  $x$  component of the Lorentz force as

$$F_x = -\frac{\partial}{\partial x} \left( e\phi - \frac{e}{c} \mathbf{v} \cdot \mathbf{A} \right) + \frac{d}{dt} \frac{\partial}{\partial v_x} \left( e\phi - \frac{e}{c} \mathbf{v} \cdot \mathbf{A} \right) \quad (1.2.26)$$

For the other  $y$  and  $z$  components of the Lorentz force, we would still obtain expressions similar to (1.2.26).

The electrostatic potential  $\phi(\mathbf{r}, t)$  is independent of velocity, and thus it is possible to just add it to the last term. The generalized potential then becomes

$$U = e\phi - \frac{e}{c} \mathbf{v} \cdot \mathbf{A} \quad (1.2.27)$$

We have found that the Lorentz force is a function of both the position and velocity of the particle. To describe the motion of the particle quantum mechanically, one needs to construct the Hamiltonian from the Lagrangian. Using  $L = T - U$  for the Lagrangian, where  $T$  and  $U$  correspond to the generalized kinetic and potential energies of the system, we obtain

$$L = \frac{1}{2} m \mathbf{v}^2 - e\phi - \frac{e}{c} \mathbf{v} \cdot \mathbf{A} \quad (1.2.28a)$$

In this problem the generalized coordinates  $q_i$  are just the Cartesian coordinates  $x, y$  and  $z$ , so that  $\dot{q}_i$  are the three components  $\mathbf{v} = (v_x, v_y, v_z)$  of the particle velocity and  $\mathbf{A} = (A_x, A_y, A_z)$  is the vector potential, where  $i = x, y, z$ .

With this knowledge we can now write

$$\mathbf{v}^2 = (v_x \hat{i} + v_y \hat{j} + v_z \hat{k}) \cdot (v_x \hat{i} + v_y \hat{j} + v_z \hat{k}) = \sum_i v_i^2 \quad (1.2.28b)$$

And

$$\mathbf{v} \cdot \mathbf{A} = (v_x \hat{i} + v_y \hat{j} + v_z \hat{k}) \cdot (A_x \hat{i} + A_y \hat{j} + A_z \hat{k}) = \sum_i v_i A_i \quad (1.2.28c)$$



Thus in terms of the generalized coordinates, the Lagrangian becomes

$$L = \frac{1}{2}m \sum_i \dot{q}_i^2 - e\phi(q_i) + \frac{e}{c} \sum_i \dot{q}_i A_i \quad (1.2.29)$$

The canonical momentum is

$$p_i = \frac{\partial L}{\partial \dot{q}_i} = m\dot{q}_i + \frac{e}{c} A_i \quad (1.2.30)$$

In vector form, (1.2.30) is written as

$$\mathbf{p} = m\mathbf{v} + \frac{e}{c} \mathbf{A} \quad (1.2.31)$$

We can now derive the Hamiltonian  $H$  of a charged particle in an electromagnetic field from the Lagrangian  $L$  by means of the Legendre transformation [2]

$$H = \sum_i p_i \dot{q}_i - L \quad (1.2.32)$$

We find that

$$H = \frac{1}{2m} \left( \mathbf{p} - \frac{e}{c} \mathbf{A} \right)^2 + e\phi \quad (1.2.33)$$

The velocity is replaced using equation (1.2.31). This equation indicates the simplest way of coupling the electric field to the motion of the charged particle.

The transition to quantum mechanics is obtained by replacing the canonical momentum  $\mathbf{p}$  by  $\left(\frac{\hbar}{i}\right) \nabla$ , according to the rules of quantization in the coordinate representation [2, 4]. Thus we obtain the Hamiltonian operator

$$\hat{H} = \frac{1}{2m} \left( \frac{\hbar}{i} \nabla - \mathbf{A} \frac{e}{c} \right)^2 + e\phi \quad (1.2.34)$$

### 1.2.2 Gauge Invariance in the Schrödinger Equation

It is well known that the electromagnetic potentials  $A$  and  $\phi$  are not unique, but are gauge dependent [2, 5]. The states of the particle in an electromagnetic field are given as solutions of the Schrödinger equation with the Hamiltonian given above in (1.2.33). The Schrödinger equation is

$$\left\{ \frac{1}{2m} \left[ \hat{p} - \frac{e}{c} A \right]^2 + e\phi \right\} \psi = i\hbar \frac{\partial}{\partial t} \psi \quad (1.2.35)$$

Gauge invariance [2] means that the solutions of the Schrödinger equation describe the same physical states if we apply to the potentials the transformations

$$A' = A + \nabla f(\mathbf{r}, t)$$

and

$$\phi' = \phi - \frac{1}{c} \frac{\partial f}{\partial t}(\mathbf{r}, t) \quad (1.2.36)$$

where the function  $f(\mathbf{r}, t)$  is arbitrary. In four-component relativistic notation introduced through the four-vector  $A_\mu$ , these transformations become

$$A'_\mu = A_\mu + \frac{\partial f}{\partial x_\mu}, \text{ with} \quad (1.2.37)$$
$$A_\mu = \{A, i\phi\} \text{ and } \mu = 1, 2, 3, 4$$

where  $x_1 = x$ ,  $x_2 = y$ ,  $x_3 = z$ ,  $x_4 = ict$ .

The Schrödinger equation corresponding to the Hamiltonian  $\hat{H}'$ , with primed potentials can be written as

$$\hat{H}' \psi' = i\hbar \frac{\partial}{\partial t} \psi' \quad (1.2.38)$$

Here, gauge invariance implies that the two solutions  $\psi$  and  $\psi'$  differ only by a phase factor. Starting with

$$\psi' = \psi \exp\left(\frac{ie}{\hbar c} f(\mathbf{r}, t)\right) \quad (1.2.39)$$

and inserting it in (1.2.38) gives

$$\begin{aligned}
 & \frac{[\hat{\mathbf{p}} - (e/c)\mathbf{A} - (e/c)\nabla f]^2}{2m} \psi \exp\left(\frac{ie}{\hbar c} f(\mathbf{r}, t)\right) + e \left( \phi - \frac{1}{c} \frac{\partial f}{\partial t}(\mathbf{r}, t) \right) \psi \exp\left(\frac{ie}{\hbar c} f(\mathbf{r}, t)\right) \\
 &= i\hbar \frac{\partial \psi}{\partial t} \exp\left(\frac{ie}{\hbar c} f(\mathbf{r}, t)\right) - \frac{e}{c} \frac{\partial f}{\partial t} \psi \exp\left(\frac{ie}{\hbar c} f(\mathbf{r}, t)\right)
 \end{aligned} \tag{1.2.40}$$

From (1.2.40), we see that

$$\begin{aligned}
 \left(\hat{\mathbf{p}} - \frac{e}{c}\mathbf{A}'\right) \psi' &= \left(\frac{\hbar}{i}\nabla - \frac{e}{c}\mathbf{A} - \frac{e}{c}\nabla f\right) \psi \exp\left(\frac{ie}{\hbar c} f(\mathbf{r}, t)\right) \\
 &= \exp\left(\frac{ie}{\hbar c} f(\mathbf{r}, t)\right) \left(\frac{\hbar}{i}\nabla + \frac{e}{c}\nabla f - \frac{e}{c}\mathbf{A} - \frac{e}{c}\nabla f\right) \psi \\
 &= \exp\left(\frac{ie}{\hbar c} f(\mathbf{r}, t)\right) \left(\frac{\hbar}{i}\nabla - \frac{e}{c}\mathbf{A}\right) \psi
 \end{aligned} \tag{1.2.41}$$

Applying the operator  $\left(\hat{\mathbf{p}} - \frac{e}{c}\mathbf{A}'\right)$  again, gives the equation

$$\hat{H}\psi = i\hbar \frac{\partial \psi}{\partial t} \tag{1.2.42}$$

The equation (1.2.42) follows from (1.2.38) by using (1.2.39). This shows that the solutions of the Schrödinger equation (1.2.35) still describe the same physical states, even after a gauge transformation. The states  $\psi_n$  and  $\psi'_n$  differ only by a unique phase factor  $\exp\left(\frac{ie}{\hbar c} f(\mathbf{r}, t)\right)$ .

This also shows that the canonical momentum  $\mathbf{p} \rightarrow -i\hbar\nabla$  is not a directly measurable quantity since its expectation value is not gauge invariant [2]. Hence, if in a physical problem the momentum operator  $\hat{\mathbf{p}}$  appears, it must always be replaced by  $\left(\hat{\mathbf{p}} - \frac{e}{c}\mathbf{A}\right)$  if electromagnetic fields are present. This will guarantee gauge invariance in the theory.

We now consider gauge invariance in relativistic notation.

The gauge transformation for the electromagnetic field is expressed by

$$\begin{aligned}
 A'_\mu &= A_\mu + \frac{\partial f}{\partial x_\mu}, \text{ with} \\
 A_\mu &= \{\mathbf{A}, i\phi\} \text{ and } x_\mu = \{\mathbf{x}, ict\}
 \end{aligned} \tag{1.2.43}$$

The four-momentum operator is given by

$$\hat{p}_\mu = -i\hbar \left\{ \frac{\partial}{\partial x_1}, \frac{\partial}{\partial x_2}, \frac{\partial}{\partial x_3}, \frac{\partial}{\partial x_4} \right\} = \left\{ \hat{\mathbf{p}}, \frac{i\hat{E}}{c} \right\} \quad (1.2.44)$$

We make use of

$$\hat{p}_\mu \rightarrow \hat{p}_\mu - \frac{e}{c} A_\mu \quad (1.2.45)$$

to achieve minimal coupling of the electromagnetic field and the particle.

Similar to (1.2.39) we have the following phase transformation of the wave function

$$\psi'(x_\mu) = \psi(x_\mu) \exp\left(\frac{ie}{\hbar c} f(x_\mu)\right) \quad (1.2.46)$$

then

$$\begin{aligned} \left(\hat{p}_\mu - \frac{e}{c} A'_\mu\right) \psi'(x_\mu) &= \left(\hat{p}_\mu - \frac{e}{c} A_\mu - \frac{e}{c} \nabla f\right) \exp\left(\frac{ie}{\hbar c} f(x_\mu)\right) \\ &= \exp\left(\frac{ie}{\hbar c} f(\mathbf{r}, t)\right) \left(\hat{p}_\mu - \frac{e}{c} A_\mu\right) \psi(x_\mu) \end{aligned} \quad (1.2.47)$$

is valid. This ensures that observables of the type

$$\begin{aligned} \langle \psi'_f(x_\mu) | V(x_\mu) | \psi'_i(x_\mu) \rangle &= \langle \psi_f(x_\mu) | V(x_\mu) | \psi_i(x_\mu) \rangle \quad \text{and} \\ \langle \psi'_f(x_\mu) | F\left(\hat{p}_\mu - \frac{e}{c} A'_\mu\right) | \psi'_i(x_\mu) \rangle &= \langle \psi_f(x_\mu) | F\left(\hat{p}_\mu - \frac{e}{c} A_\mu\right) | \psi_i(x_\mu) \rangle \end{aligned} \quad (1.2.48)$$

are invariant under the gauge transformations. The equations in (1.2.47) are exactly the right-hand sides of the equations (1.2.40) for  $\mu = 4$  and (1.2.41) for  $\mu = 1, 2, 3$  respectively.

### 1.2.3 Gauge Invariance in Hamilton's Equations

The gauge invariance of Hamilton's equations [2] is discussed by considering the generalized position coordinates  $q_1, q_2, \dots, q_f$  and the canonical conjugated momenta  $p_1, p_2, \dots, p_f$ .

The Hamiltonian  $H$  is a function of those coordinates and momenta, and, in general, of the time.

The Hamilton equations are

$$\frac{dp_i}{dt} = -\frac{\partial H}{\partial q_i}, \quad \frac{dq_i}{dt} = \frac{\partial H}{\partial p_i} \quad (1.2.49)$$

From section (1.2.1), we recall that total time derivative of any function  $F(p_i, q_i, t)$  of the generalized coordinates and momenta is expressed as

$$\frac{dF}{dt} = \frac{\partial F}{\partial t} + \sum_{i=1}^f \left( \frac{\partial F}{\partial q_i} \dot{q}_i + \frac{\partial F}{\partial p_i} \dot{p}_i \right) \quad (1.2.50)$$

By using Hamilton's equations (1.2.49), the second term on the right-hand side of (1.2.50) can be written as

$$\sum_{i=1}^f \left( \frac{\partial F}{\partial q_i} \dot{q}_i + \frac{\partial F}{\partial p_i} \dot{p}_i \right) = \sum_{i=1}^f \left( \frac{\partial F}{\partial q_i} \frac{\partial H}{\partial p_i} - \frac{\partial F}{\partial p_i} \frac{\partial H}{\partial q_i} \right) \equiv \{F, H\},$$

and, hence, (1.2.50) becomes

$$\frac{dF}{dt} = \frac{\partial F}{\partial t} + \{F, H\} \quad (1.2.51)$$

where  $\{F, H\}$  is called the Poisson bracket and is equal to

$$\{F, H\} = \sum_{i=1}^f \left( \frac{\partial F}{\partial q_i} \frac{\partial H}{\partial p_i} - \frac{\partial F}{\partial p_i} \frac{\partial H}{\partial q_i} \right) \quad (1.2.52)$$

Hamilton's equations can now be written as

$$\frac{dp_i}{dt} = \{H, p_i\}, \quad \frac{dq_i}{dt} = \{H, q_i\}, \quad i = 1, 2, \dots, f \quad (1.2.53)$$

The equations of motion are also written in the same way [2]. In the special case of a Cartesian system and of a particle in a force field derivable from a potential function  $V(x, y, z, t)$ , we have

$$H = \frac{1}{2m} (p_x^2 + p_y^2 + p_z^2) + V(x, y, z, t) \quad (1.2.54)$$

where  $q_1 = x$ ,  $q_2 = y$ ,  $q_3 = z$ , and  $p_1 = p_x$ ,  $p_2 = p_y$  and  $p_3 = p_z$ . Using (1.2.53) we obtain

$$\frac{dp_x}{dt} = \{H, p_x\} = -\frac{\partial H}{\partial x} = -\frac{\partial V}{\partial x},$$

$$\frac{dp_y}{dt} = \{H, p_y\} = -\frac{\partial H}{\partial y} = -\frac{\partial V}{\partial y},$$

$$\frac{dp_z}{dt} = \{H, p_z\} = -\frac{\partial H}{\partial z} = -\frac{\partial V}{\partial z},$$

$$\frac{dx}{dt} = \{H, x\} = \frac{\partial H}{\partial p_x} = \frac{p_x}{m},$$

$$\frac{dy}{dt} = \{H, y\} = \frac{\partial H}{\partial p_y} = \frac{p_y}{m},$$

$$\frac{dz}{dt} = \{H, z\} = \frac{\partial H}{\partial p_z} = \frac{p_z}{m} \quad (1.2.55)$$

From (1.2.55) we get

$$m \frac{d^2x}{dt^2} = -\frac{\partial V}{\partial x},$$

$$m \frac{d^2y}{dt^2} = -\frac{\partial V}{\partial y},$$

$$m \frac{d^2z}{dt^2} = -\frac{\partial V}{\partial z} \quad (1.2.56)$$

These are just one dimensional Newton's equations of motion.

In the case of the motion of a charged particle with charge  $e$  and mass  $m$  in an electromagnetic field described by the potential  $\phi = 1/e V(x, t)$  and vector potential  $A$ , we have

$$\mathbf{E} = -\nabla\phi - \frac{1}{c} \frac{\partial \mathbf{A}}{\partial t},$$

$$\mathbf{B} = \nabla \times \mathbf{A} \quad (1.2.57)$$

where  $\mathbf{E}$  and  $\mathbf{B}$  are the electric and magnetic fields. In this case the Hamiltonian function can be written as

$$H = \frac{1}{2m} \left( p - \frac{e}{c} A \right)^2 + e\phi \quad (1.2.58)$$

which is equivalent to equation (1.2.34).

We can show that the Hamilton equations that emerge from the Hamiltonian expressed by (1.2.58) are equivalent to Newton's equations of motion of the same particle under the influence of the Lorentz force. These are

$$\begin{aligned}
 m \frac{d^2 \mathbf{r}}{dt^2} &= e \left( \mathbf{E} + \frac{1}{c} \mathbf{v} \times \mathbf{B} \right), \\
 m \frac{d^2 x}{dt^2} &= e \left( E_x + \frac{1}{c} \left( \frac{dy}{dt} B_z - \frac{dz}{dt} B_y \right) \right), \\
 m \frac{d^2 y}{dt^2} &= e \left( E_y + \frac{1}{c} \left( \frac{dz}{dt} B_x - \frac{dx}{dt} B_z \right) \right), \\
 m \frac{d^2 z}{dt^2} &= e \left( E_z + \frac{1}{c} \left( \frac{dx}{dt} B_y - \frac{dy}{dt} B_x \right) \right)
 \end{aligned} \tag{1.2.59}$$

Inserting  $H$  from (1.2.58) into the general definition of the Hamilton equations (1.2.53) leads to the expression

$$\frac{dp_x}{dx} = \frac{e}{mc} \left( \left( p_x - \frac{e}{c} A_x \right) \frac{\partial A_x}{\partial x} + \left( p_y - \frac{e}{c} A_y \right) \frac{\partial A_y}{\partial y} + \left( p_z - \frac{e}{c} A_z \right) \frac{\partial A_z}{\partial z} \right) - e \frac{\partial \phi}{\partial x} \tag{1.2.60}$$

and

$$\begin{aligned}
 \frac{dx}{dt} &= \frac{1}{m} \left( p_x - \frac{e}{c} A_x \right), \\
 \frac{dy}{dt} &= \frac{1}{m} \left( p_y - \frac{e}{c} A_y \right), \\
 \frac{dz}{dt} &= \frac{1}{m} \left( p_z - \frac{e}{c} A_z \right),
 \end{aligned} \tag{1.2.61}$$

Considering only the first of equations (1.2.61), we see that the total time derivative of the momentum can now be written as

$$\frac{dp_x}{dt} = m \frac{d^2 x}{dt^2} + \frac{e}{c} \frac{dA_x}{dt} \tag{1.2.62}$$

Thus (1.2.60) can now be written in the following form:

$$m \frac{d^2 x}{dt^2} + \frac{e}{c} \frac{dA_x}{dt} = \frac{e}{c} \left( \frac{dx}{dt} \frac{\partial A_x}{\partial x} + \frac{dy}{dt} \frac{\partial A_y}{\partial x} + \frac{dz}{dt} \frac{\partial A_z}{\partial x} \right) - e \frac{\partial \phi}{\partial x} \tag{1.2.63}$$

## Chapter 1. Introduction

---

Since the value of the vector potential  $\mathbf{A}$  is obtained at the position of the charge  $e$ , the total derivative of  $A_x$  with respect to time is

$$\frac{dA_x}{dt} = \frac{\partial A_x}{\partial t} + \frac{\partial A_x}{\partial x} \frac{dx}{dt} + \frac{\partial A_x}{\partial y} \frac{dy}{dt} + \frac{\partial A_x}{\partial z} \frac{dz}{dt} \quad (1.2.64)$$

Now substituting equation (1.2.64) into equation (1.2.63) and rearranging gives

$$m \frac{d^2 x}{dt^2} = -\frac{e}{c} \frac{\partial A_x}{\partial t} - \frac{e}{c} \left( \frac{dy}{dt} \left( \frac{\partial A_y}{\partial x} - \frac{\partial A_x}{\partial y} \right) + \frac{dz}{dt} \left( \frac{\partial A_z}{\partial x} - \frac{\partial A_x}{\partial z} \right) \right) - e \frac{\partial \phi}{\partial x} \quad (1.2.65)$$

Using the equations (1.2.57) which connect the fields and the potentials we get

$$m \frac{d^2 x}{dt^2} = e \left( E_x + \frac{1}{c} \left( \frac{dy}{dt} B_z - \frac{dz}{dt} B_y \right) \right) \quad (1.2.66)$$

This is the first of the equations (1.2.59); the other two can be derived in the same way. This shows that the Hamilton equations resulting from the Hamiltonian (1.2.58) are equivalent to Newton's equations (1.2.59). Thus the potentials  $\mathbf{A}$  and  $\phi$  can be chosen at will, as long as the equations (1.2.57) give the required electromagnetic field. Using  $\mathbf{A}'$  and  $\phi'$  instead of  $\mathbf{A}$  and  $\phi$ , such that

$$\mathbf{A}' = \mathbf{A} + \nabla f(\mathbf{r}, t)$$

and

$$\phi' = \phi - \frac{1}{c} \frac{\partial f}{\partial t}(\mathbf{r}, t) \quad (1.2.67)$$

with  $f$  defined as an arbitrary function of the position coordinates and time. Then  $\mathbf{E}' = \mathbf{E}$  and similarly,  $\mathbf{B}' = \mathbf{B}$ . If we replace  $\mathbf{A}$  and  $\phi$  in the Hamiltonian (1.2.58) by  $\mathbf{A}'$  and  $\phi'$ , we obtain the equation of motion (1.2.63), i.e., the same equation as (1.2.59). Thus, it has been shown by using (1.2.67) that the equations (1.2.59) are independent of the choice of the potentials. This property of the Hamiltonian equations is known as *gauge invariance*.

### 1.2.4 Gauge Dependence of the Canonical Momentum

For the Schrodinger equation to remain unchanged under a gauge transformation, the wave function  $\psi(\mathbf{r}, t)$  must change into  $\psi'(\mathbf{r}, t) = \exp\left(\frac{ie}{\hbar c} f(\mathbf{r}, t)\right) \psi(\mathbf{r}, t)$ . This corresponds to a



phase change, which varies from one point to another. It is thus not a global phase factor. For the state vector we have

$$\begin{aligned} |\psi'(t)\rangle &= \exp\left(\frac{ie}{\hbar c} f(\mathbf{r}, t)\right) |\psi(t)\rangle \\ &= G |\psi(t)\rangle \end{aligned} \quad (1.2.68)$$

Here,

$$G = \exp\left(\frac{ie}{\hbar c} f(\mathbf{r}, t)\right) \quad (1.2.69)$$

Now, in order for the behavior of an observable  $A$  to be invariant under a gauge transformation we need

$$\langle \psi' | A | \psi' \rangle = \langle \psi | A | \psi \rangle,$$

or

$$G^\dagger A G = A \quad (1.2.70)$$

A true physical quantity is an observable for which (1.2.70) is true. The observable  $\mathbf{r}$  is such a true physical quantity. For the canonical momentum  $\mathbf{p}$  we have

$$G^\dagger \mathbf{p} G = G^\dagger \mathbf{p} G - G^\dagger G \mathbf{p} + \mathbf{p} = G^\dagger [\mathbf{p}, G] + \mathbf{p} \quad (1.2.71)$$

Now substituting (1.2.69) into (1.2.71) gives

$$\begin{aligned} G^\dagger \mathbf{p} G &= \exp\left(-\frac{ie}{\hbar c} f(\mathbf{r}, t)\right) [\mathbf{p}, G] + \mathbf{p} = -\exp\left(\frac{ie}{\hbar c} f(\mathbf{r}, t)\right) i\hbar \nabla \exp\left(\frac{ie}{\hbar c} f(\mathbf{r}, t)\right) + \mathbf{p} \\ &= \mathbf{p} + \frac{e}{c} \nabla f \end{aligned} \quad (1.2.72)$$

where we have used the relation  $[p, G(x)] = -i\hbar G'(x)$ .

From (1.2.72) we conclude that the canonical momentum is gauge dependent and hence is not a true physical quantity. However, the mechanical momentum  $\mathbf{p}_{mech} = \mathbf{p} - \frac{e}{c} \mathbf{A}$  is gauge invariant [2], so that

$$G^\dagger \left( \mathbf{p} - \frac{e}{c} \mathbf{A} - \frac{e}{c} \nabla f \right) G = \mathbf{p} - \frac{e}{c} \mathbf{A} \quad (1.2.73)$$

### 1.2.5 Gauge Fixing in Classical Gauge Theories

In classical electromagnetism, the **gauge-fixing** problem is simply the problem of choosing a representative in the class of equivalent potentials, convenient for practical calculations or most suited to physical intuition. Among the most common non-relativistic gauges, one may cite:

- $\nabla \cdot \mathbf{A}(\mathbf{r}, t) = 0$ , known as Coulomb's gauge,
- $A_0(\mathbf{r}, t) = 0$ ,  $\phi = 0$ , known as the temporal gauge (or Hamiltonian or Weyl's gauge),
- $\mathbf{n} \cdot \mathbf{A}(\mathbf{r}, t) = 0$ , known as the non – relativistic axial gauge,
- $\mathbf{x} \cdot \mathbf{A}(\mathbf{r}, t) = 0$ , known as the multipolar or non – relativistic Poincaré gauge, and the relativistically invariant gauge:
- $\sum_\mu \partial^\mu A_\mu(x) = 0$ , known as the Lorentz or Landau gauge,
- $\sum_\mu x^\mu A_\mu(x) = 0$ , known as the relativistic Poincaré or Fock – Schwinger gauge,
- $\sum_\mu n^\mu A_\mu(x) = 0$ ,  
when  $n$  is a space – like quadrivector, is known as the relativistic axial gauge,
- $\sum_\mu n^\mu A_\mu(x) = 0$ , when  $n$  is a null – like quadrivector, is known as the light – cone gauge,
- $\sum_\mu \partial^\mu A_\mu(x) = s(x)$ , for some scalar function  $s(x)$  (this gauge is sometimes used in the quantization process).

However, some of these conditions do not fix the gauge field representative completely [6]. The form and the meaning of the residual invariance depend on the gauge fixed. Finally, these gauges have simple generalizations to the non-Abelian situation [6].

## 1.3 The Density Functional Theory

Most electronic structure calculations for solids are based on the density functional theory (DFT), which results from the work of Hohenberg, Kohn and Sham [7, 8]. This approach has become very popular for atoms, molecules and solids [9]. In density functional theory, the electronic orbitals are solutions to a Schrödinger equation that depends on the electron density rather than on the individual orbitals [9]. The dependence of the one-particle Hamiltonian on this density is in principle non-local [9, 10]. Often, this Hamiltonian is assumed to depend on the local value of the density only; this is the local density approximation (LDA) [9]. In the vast majority of DFT electronic structure calculations, this approximation is adopted [10]. It is also applied to atomic and molecular systems [11].

### 1.3.1 Physical picture - Hohenberg-Kohn theorems

In their work [7], Hohenberg and Kohn established that for any system of interacting particles moving under the influence of an external potential:

- The external potential  $V_{ext}$ , is uniquely determined by the ground state particle density  $n(\mathbf{r})$ ; in the sense that, there cannot be two potentials that differ by more than a constant and that give rise to the same ground state density. Thus, since the external potential defines the Hamiltonian and therefore the many-body wave function, all properties of the system are uniquely determined by its ground state density.
- An energy functional  $E[n]$  exists, such that the exact ground state energy is given by the global minimum of the energy functional  $E[n]$ , and the ground state density is the density that minimizes  $E[n]$ .

The above statements constitute the Hohenberg-Kohn theorems and are the basis of all density functional calculations [9].

Assuming that the full wave function of an electron gas moving under the influence of an external potential and mutual coulomb repulsion can be approximated as

$$\Psi(\mathbf{r}_1, \mathbf{r}_2, \dots, \mathbf{r}_N) = \psi_1(\mathbf{r}_1)\psi_2(\mathbf{r}_2) \dots \psi_N(\mathbf{r}_N) \quad (1.3.0)$$

with  $N$  being the total number of electrons in the system, we can write the electronic density as

$$n(\mathbf{r}) = \sum_N |\psi(\mathbf{r}_N)|^2 \quad (1.3.1)$$

and the Hamiltonian in the form

$$\hat{H} = \hat{T} + \hat{V}_{ee} + \hat{V}_{ext} \quad (1.3.2)$$

where  $\hat{T}$ ,  $\hat{V}_{ee}$  and  $\hat{V}_{ext}$  are the kinetic, interaction and external potential energies.

Now, from the variational principle, if we minimize (1.3.2) over all  $\Psi$  in the ground state that give the same  $n(\mathbf{r})$  we get the ground state energy  $E_{GS}$  given by the expression

$$E_{GS} = \min_{\Psi} [\langle \Psi | \hat{H} | \Psi \rangle] = \min_{\Psi} [\langle \Psi | \hat{T} + \hat{V}_{ee} + \hat{V}_{ext} | \Psi \rangle] \quad (1.3.3a)$$

The operators  $\hat{T}$  and  $\hat{V}_{ee}$  are universal operators as they are the same for any  $N$ -electron system, while  $\hat{V}_{ext}$  is system dependent.

We then write the contribution of the external potential  $\langle \Psi | \hat{V}_{ext} | \Psi \rangle$  in terms of the ground state density  $n(\mathbf{r})$  as

$$\hat{V}_{ext} = \int d^3r n(\mathbf{r}) \hat{V}_{ext} \quad (1.3.3b)$$

Again, by the variational principle, varying  $n(\mathbf{r})$  in (1.3.3a) leads to

$$E_{GS} = \min_n \left[ \min_{\Psi \rightarrow n} [\langle \Psi | \hat{T} + \hat{V}_{ee} | \Psi \rangle] + \int d^3r n(\mathbf{r}) \hat{V}_{ext} \right] \quad (1.3.4)$$

Now, since  $\Psi$  is a functional of  $n(\mathbf{r})$ , so is evidently the kinetic and interaction energy, we therefore define  $F[n]$  as a universal functional of  $n(\mathbf{r})$  by the expression

$$F[n] = \min_{\Psi \rightarrow n} [\langle \Psi | \hat{T} + \hat{V}_{ee} | \Psi \rangle] = \langle \Psi_n | \hat{T} + \hat{V}_{ee} | \Psi_n \rangle \quad (1.3.5)$$

Then,

$$E_{GS} = \min_n \left[ F[n] + \int d^3r n(\mathbf{r}) \hat{V}_{ext} \right] \quad (1.3.6)$$

and

$$E[n] = \left[ F[n] + \int d^3r n(\mathbf{r}) \hat{V}_{ext} \right] \quad (1.3.7)$$

$E[n]$  assumes its minimum value for the correct  $n(\mathbf{r})$ , if

$$N[n] = \int d^3r n(\mathbf{r}) = N \quad (1.3.8)$$

Thus, the variational equation for  $n(\mathbf{r})$  is

$$\frac{\delta}{\delta n(\mathbf{r})} \left\{ F[n] + \int d^3r n(\mathbf{r}) \hat{V}_{ext} - \mu \left( \int d^3r n(\mathbf{r}) - N \right) \right\} = 0$$

$$\left. \frac{\delta F[n]}{\delta n(\mathbf{r})} \right|_{n=n_{GS}} + \{ \hat{V}_{ext}(\mathbf{r}) - \mu \} = 0 \quad (1.3.9)$$

Implying that

$$\hat{V}_{ext}(\mathbf{r}) = \mu - \left. \frac{\delta F[n]}{\delta n(\mathbf{r})} \right|_{n=n_{GS}} \quad (1.3.10)$$

where  $\mu$  is a Lagrange parameter [8] to enforce the restrictive condition (1.3.8). Equation (1.3.10) shows that  $\hat{V}_{ext}(\mathbf{r})$  is to within a constant a unique functional of the electronic density and thus proves the first Hohenberg-Kohn theorem.

The equation (1.3.7) proves the first part of the second theorem; the energy functional  $E[n]$  exists, and that the ground state energy can be obtained by minimizing some density functional. It also “defines” the functional that has to be minimized. In what remains, we show that the density that minimizes  $E[n]$  is also the ground state density.

If we denote the Hamiltonian and ground state energies associated with  $\Psi_{GS}$  and  $\Psi_{n_{GS}}$  by  $H_{GS}, H_{n_{GS}}$  and  $E_{GS}, E_{n_{GS}}$ , we have by the minimal property of the ground state [7]

$$E_{GS} = [\langle \Psi_{GS} | \hat{T} + \hat{V}_{ee} + \hat{V}_{ext} | \Psi_{GS} \rangle] \leq [\langle \Psi_{n_{GS}} | \hat{T} + \hat{V}_{ee} + \hat{V}_{ext} | \Psi_{n_{GS}} \rangle] \quad (1.3.11)$$

where  $n_{GS}$  is the ground state density and  $\Psi_{GS}$  the ground state wave function. If we assume a non-degenerate ground state

$$\Psi_{GS} = \Psi_{n_{GS}} \quad (1.3.12)$$

$$E_{GS} = [\langle \Psi_{n_{GS}} | \hat{T} + \hat{V}_{ee} + \hat{V}_{ext} | \Psi_{n_{GS}} \rangle] = [\langle \Psi_{n_{GS}} | \hat{T} + \hat{V}_{ee} | \Psi_{n_{GS}} \rangle] + \int d^3r n_{GS}(\mathbf{r}) \hat{V}_{ext}$$

$$E_{GS} = \left[ F[n_{GS}] + \int d^3r n_{GS}(\mathbf{r}) \hat{V}_{ext} \right]$$

$$E_{GS} = \min_n \left[ F[n] + \int d^3r n(\mathbf{r}) \hat{V}_{ext} \right] \quad (1.3.13)$$

Here, we have used equation (1.3.10). This shows that  $E[n]$  is indeed minimized by the correct ground state density. (1.3.13) completes the proof of the second theorem.

We note that, if  $F[n]$  were a known and sufficiently simple functional of the density  $n(\mathbf{r})$ , the problem of determining the ground state energy and density in a given external potential would be rather easy since it requires merely the minimization of a functional of the density functional. The major parts of the complexities of the many-electron problem are thus associated with the universal functional  $F[n]$ .

### 1.3.2 The Kohn-Sham equations: Exchange and correlation effects

Because coulomb interactions have a long range, it is usually convenient to separate out from  $F[n]$  the classical energy and write

$$F[n] = \frac{1}{2} \iint d^3r d^3r' \frac{n(\mathbf{r})n(\mathbf{r}')}{|\mathbf{r} - \mathbf{r}'|} + G[n] \quad (1.3.14)$$

## Chapter 1. Introduction

---

The first term on the right hand side of (1.3.14) corresponds to the Hartree energy and is considered to be the largest part of the interaction energy [9] and the second term  $G[n]$ , is a universal functional of the density  $n(\mathbf{r})$  just like  $F[n]$ . Here, we consider an approximation for  $G[n]$  which leads to a scheme analogous to the Hartree - Fock method. The aim is to approximate the kinetic energy of the interacting system by the kinetic energy of a non-interacting (hypothetical) system with the same electronic density as the interacting system.

We first write

$$G[n] = T_0[n] + E_{xc}[n] \quad (1.3.15)$$

where  $T_0[n]$  is the kinetic energy of the a system of non-interacting electrons with density  $n(\mathbf{r})$  and  $E_{xc}[n]$  is, by definition, the exchange and correlation energy of an interacting system with density  $n(\mathbf{r})$ .

The energy functional for a many-electron system can now be written as

$$E[n] = T_0[n] + \int d^3r n(\mathbf{r}) \left( V_{ext} + \frac{1}{2} V_H \right) + E_{xc}[n] \quad (1.3.16)$$

Here,  $V_H$  is the Hartree potential and is given by

$$V_H = \int d^3r' \frac{n(\mathbf{r}')}{|\mathbf{r} - \mathbf{r}'|} \quad (1.3.17)$$

Now, for the non-interacting hypothetical system, an effective potential has to be chosen such that its density is equal to the density of the interacting system. With this in mind, the energy functional of the non-interacting system can be written as

$$E_0[n] = T_0[n] + \int d^3r n(\mathbf{r}) V_{eff}(\mathbf{r}) \quad (1.3.18)$$

where  $V_{eff}(\mathbf{r})$  is the effective potential energy of the system.

## Chapter 1. Introduction

---

In the previous section, it was shown that the ground state of the many-electron system can be found by minimizing the energy functional  $E[n]$  with respect to the density, subject to the constraint (1.3.8).

The ground state density is given by

$$n(\mathbf{r}) = \sum_i |\psi_i(\mathbf{r})|^2 \quad (1.3.19)$$

Here, it is assumed that the spin orbitals  $\psi_i$  are normalized so that the density satisfies the correct normalization to the total number of particles  $N$ .

For the interacting system, we now have the variational equation

$$\frac{\delta}{\delta n(\mathbf{r})} \left[ E[n] + \mu \left( \int d^3r n(\mathbf{r}) - N \right) \right]_{n=n_{GS}} = 0 \quad (1.3.20)$$

A substitution of (1.3.16) into (1.3.20) gives

$$\frac{\delta T_0[n]}{\delta n(\mathbf{r})} + V_{ext} + V_H + \frac{\delta E_{xc}[n]}{\delta n(\mathbf{r})} = \mu \quad (1.3.21)$$

In the same way, for the non-interacting system we have

$$\frac{\delta T_0[n]}{\delta n(\mathbf{r})} + V_{eff}(\mathbf{r}) = \mu \quad (1.3.22)$$

Eliminating the kinetic energy term in (1.3.22) using (1.3.21) gives the effective potential of the non-interacting system as

$$V_{eff}(\mathbf{r}) = V_{ext}(\mathbf{r}) + V_H[n(\mathbf{r})] + \frac{\delta E_{xc}[n]}{\delta n(\mathbf{r})} \quad (1.3.23)$$

The Schrodinger equation for the many-electron non-interacting system can now be written as



$$\left[ -\frac{1}{2} \nabla^2 + V_{eff}(\mathbf{r}) \right] \psi_i(\mathbf{r}) = \varepsilon_i \psi_i(\mathbf{r}) \quad (1.3.24)$$

The equations (1.3.19), (1.3.23) and (1.3.24) constitute the Kohn-Sham system of equations and are solved self-consistently by iteration to calculate the ground state density of the original interacting problem.

The total energy of the interacting system is given by

$$\begin{aligned} E &= T_0[n] + \int d^3r n(\mathbf{r}) \left( V_{ext} + \frac{e^2}{2} V_H \right) + E_{xc}[n] \\ &= \sum \varepsilon_i[n] - \frac{e^2}{2} \iint d^3r d^3r' \frac{n(\mathbf{r})n(\mathbf{r}')}{|\mathbf{r} - \mathbf{r}'|} + E_{xc}[n] - \int d^3r n(\mathbf{r}) \frac{\delta E_{xc}[n]}{\delta n(\mathbf{r})} \end{aligned} \quad (1.3.25)$$

If a suitable approximation for the exchange correlation energy  $E_{xc}[n]$  can be found, we can calculate the ground state energy, the ground state density and any observable that is known to be an explicit functional of the density.

### 1.3.3 The Local Density Approximation

The exchange correlation function used in the density functional approximation is a functional derivative of the exchange correlation energy with respect to the local density, and for a homogeneous electron gas, this will depend on the value of the electron density. For a non-homogeneous system, the value of the exchange correlation potential at the point  $\mathbf{r}$  depends not only on the value of the density at  $\mathbf{r}$  but also on its variation close to  $\mathbf{r}$ , and it can therefore be written as an expansion in the gradients to arbitrary order of the density:

$$V_{xc}[n(\mathbf{r})] = V_{xc}[n(\mathbf{r}), \nabla n(\mathbf{r}), \nabla(\nabla n(\mathbf{r})), \dots] \quad (1.3.26)$$

The exact form of the energy functional is unknown, and the inclusion of the density gradients makes the solution of the density functional equations very complicated. Usually, to solve the many-electron problem, it is assumed that the exchange correlation energy leads to an exchange correlation potential depending on the value of the density in  $\mathbf{r}$  only and not on its gradients – this is the *local density approximation* (LDA) and is written symbolically as

$$E_{xc}^{LDA} = \int d^3r \epsilon_{xc} [n(\mathbf{r})] n(\mathbf{r}) \quad (1.3.27)$$

where  $\epsilon_{xc} [n(\mathbf{r})]$  is the exchange correlation energy per particle of a homogeneous electron gas at the density  $n$ . The LDA is exact for a homogeneous electron gas, and so it works well for systems in which the electron density does not vary too rapidly. The exchange effects are usually included in a term based on calculations for the homogeneous electron gas.

For open-shell systems the spin-up and spin-down densities  $n_+$  and  $n_-$  are usually taken into account as two independent densities in the exchange correlation energy according to a natural extension of the DFT formalism. In LDA, the exchange energy is given as

$$E_{xc}^{LDA} [n_+ n_-] = -const. \int d^3r \epsilon_{xc} [n_+^{3/4}(\mathbf{r}) + n_-^{3/4}(\mathbf{r})] n(\mathbf{r}) \quad (1.3.28)$$

where  $const. = 3/4(3/4\pi)^{1/3}$ . As expected for an exchange coupling [12], this expression contains interactions between parallel spin pairs only.

In addition to exchange, there is a contribution from the dynamical correlation effects due to the Coulomb interactions between the electrons. These are present in the exchange correlation potential, and several local density parameterizations of this interaction have been proposed. A successful one is a parameterization of the correlation energy obtained in quantum Monte Carlo simulations [12] of the homogeneous electron gas at different densities.

The DFT-LDA approach has turned out to be very successful and has led to important improvements in calculations of the physical properties of solids.

### 1.3.4 The Generalized Gradient Approximation

Research on the ways to improve exchange-correlation functionals has led to improved accuracy in results obtained using DFT calculations. Going beyond the local density approximation, the generalized gradient approximations are obtained by adding gradient terms of the electron density to the exchange-correlation energy or its corresponding potential. The second-order generalized gradient approximation to the exchange-correlation energy is written as

$$E_{xc}^{GGA} = \int d^3r \epsilon_{xc} \left( n(\mathbf{r}), \nabla n(\mathbf{r}), \nabla(\nabla n(\mathbf{r})) \right) \quad (1.3.29)$$

There are various flavors of the generalized gradient approximation (GGA); the one by Perdew, Burke and Ernzerhof (PBE) is the recommended option for use in most calculations [12]. A recent version called meta-GGA uses for the evaluation of the exchange-correlation energy both the gradient of the density and the kinetic energy density [12].

In comparison to local density approximations, generalized gradient approximations lead to improved calculations of bond angles, lengths, and energies for atoms and molecules but show only partial improvements for solids [12].

### 2.0 Algebraic Solutions of the Landau Problem

---

#### 2.1 Introduction

Exact solutions of variations of the Landau problem are rarely feasible [2]. In this chapter, we lay the foundation for the development of a computational solution of the Landau problem. We review the algebraic solutions of the ordinary Landau problem and the Landau problem with a linear potential added; in an infinite-plane and in a half-plane as is presented by Govaerts *et al* [5]. This linear potential may correspond to a constant electric field or a gravitational potential if the plane of motion is tilted with respect to the horizontal direction by some angle  $\alpha$ .

The geometry on which the motion occurs is also now known to influence the solution of the Landau problem [5]. For the case of motion in the infinite  $(x, y)$  plane with a linear potential acting in the  $y$  direction, the energy eigenstates obtained by diagonalizing the Hamiltonian of the quantum system are localized only in the  $y$  direction, while they are totally delocalized in the  $x$  direction. As such, they are non-normalizable. The probability density of these states looks like a series of  $(n+1)$  parallel stripes parallel to the  $y$  axis with exponentially smooth edges and invariant under translation along the  $x$ -axis. The energy spectrum is unbounded even though both the classical and quantum systems remain stable because the magnetic force combines with the constant force related to the linear potential added to keep the particle rotating periodically around a magnetic centre that moves at a constant velocity along the  $x$ -axis.

The motion of the particle is finally studied on a half-plane where the unboundedness of the energy spectrum of the infinite-plane is avoided by altering the geometry of the plane of motion; this is achieved by restricting the value of the  $y$  in the  $y$ -axis. The particle then remains confined in the half-plane. The resolution of the problem leads to the parabolic cylinder equations whose solutions are the parabolic cylinder functions.

## 2.2 The Ordinary Landau Problem

Consider a charged particle of mass  $m$  moving in a plane described by the Cartesian coordinates  $(x, y)$  and subject to a perpendicular homogenous magnetic field, whose direction defines the  $z$ -axis. The magnetic field derives from a vector potential, whose components in the symmetric gauge are  $(A_x(x, y) = -1/2By, A_y(x, y) = 1/2Bx)$ .

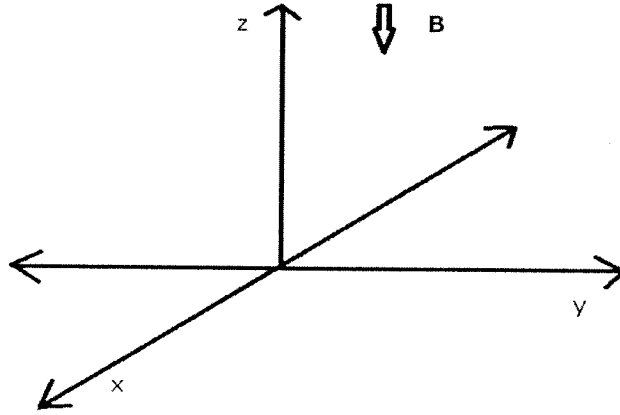


Fig.2.2: Diagram specifying the geometry of the problem

The Lagrangian

$$L = \frac{1}{2}m(\dot{x}^2 + \dot{y}^2) - \frac{1}{2}qB(\dot{x}y - x\dot{y}) - \frac{1}{2}m\omega_c^2(x^2 + y^2) \quad (2.2.0)$$

specifies the dynamics of this system through the variational principle [4]. The last term in the Lagrangian represents a symmetric potential of angular frequency  $\omega_c > 0$ . The expressions for the canonical momenta are

$$P_x = \frac{\partial L}{\partial \dot{x}} = m\dot{x} - \frac{1}{2}qBy, \quad P_y = \frac{\partial L}{\partial \dot{y}} = m\dot{y} + \frac{1}{2}qBx \quad (2.2.1)$$

Thus the velocities in the  $x$  and  $y$  directions are

$$\dot{x} = \frac{1}{m} \left( P_x + \frac{1}{2}qBy \right), \quad \dot{y} = \frac{1}{m} \left( P_y - \frac{1}{2}qBx \right) \quad (2.2.2)$$

From the Lagrangian we can now derive the Hamiltonian using the Legendre transformation

$$H = \dot{x}P_x + \dot{y}P_y - L \quad (2.2.3)$$

Substituting the equations (2.2.0) and (2.2.2) into (2.2.3) yields

$$H = \frac{1}{2m}(P_x^2 + P_y^2) + \frac{1}{2}m\left(\omega_c^2 + \left(\frac{qB}{2m}\right)^2\right)(x^2 + y^2) - \frac{qB}{2m}(xP_y - yP_x) \quad (2.2.4)$$

We now introduce the Cartesian Fock raising and lowering operators,

$$a_x = \frac{1}{2}\sqrt{\frac{m\omega_c}{\hbar}}\left(\hat{x} + \frac{i}{m\omega_c}\hat{p}_x\right), \quad a_x^\dagger = \frac{1}{2}\sqrt{\frac{m\omega_c}{\hbar}}\left(\hat{x} - \frac{i}{m\omega_c}\hat{p}_x\right)$$

$$a_y = \frac{1}{2}\sqrt{\frac{m\omega_c}{\hbar}}\left(\hat{y} + \frac{i}{m\omega_c}\hat{p}_y\right), \quad a_y^\dagger = \frac{1}{2}\sqrt{\frac{m\omega_c}{\hbar}}\left(\hat{y} - \frac{i}{m\omega_c}\hat{p}_y\right) \quad (2.2.5)$$

which satisfy the commutation relations

$$[a_x, a_x^\dagger] = 1 = [a_y, a_y^\dagger], \quad \omega_c = \frac{qB}{m} \quad (2.2.6)$$

Substitution of the inverse relations of (2.2.5) into (2.2.4) produces the Hamiltonian

$$H = \frac{1}{2}\hbar\omega_c[a_x^\dagger a_x + a_y^\dagger a_y + 1] + \frac{1}{2}i\hbar\omega_c[a_x^\dagger a_x - a_y^\dagger a_y] \quad (2.2.7)$$

Next, we introduce the chiral raising and lowering operators,

$$a_{\pm} = \frac{1}{\sqrt{2}}(a_x \mp i a_y), \quad a_{\pm}^{\dagger} = \frac{1}{\sqrt{2}}(a_x^{\dagger} \pm i a_y^{\dagger}) \quad (2.2.8)$$

satisfying the commutation relations

$$[a_{\pm}, a_{\pm}^{\dagger}] = 1, \quad [a_{\pm}, a_{\mp}^{\dagger}] = 0 \quad (2.2.9)$$

A substitution of (2.2.8) into the Hamiltonian (2.2.7) yields

$$H = \hbar\omega_c \left( a_{-}^{\dagger} a_{-} + \frac{1}{2} \right) \quad (2.2.10)$$

It is clear that the states of the system are given by the orthonormalized Fock state basis  $|n_{-}\rangle$ . Hence the Hamiltonian (2.2.10) diagonalizes as

$$H|n_{-}\rangle = E(n_{-})|n_{-}\rangle \quad (2.2.11)$$

$$\begin{aligned} \hbar\omega_c \left( a_{-}^{\dagger} a_{-} + \frac{1}{2} \right) |n_{-}\rangle &= \hbar\omega_c \left( a_{-}^{\dagger} a_{-} |n_{-}\rangle + \frac{1}{2} |n_{-}\rangle \right) = \hbar\omega_c \left( n_{-} |n_{-}\rangle + \frac{1}{2} |n_{-}\rangle \right) \\ &= \hbar\omega_c \left( n_{-} + \frac{1}{2} \right) |n_{-}\rangle \end{aligned} \quad (2.2.12)$$

Here we have used

$$\begin{aligned} a_{-} |n_{-}\rangle &= \sqrt{n_{-}} |n_{-} - 1\rangle, \quad a_{-}^{\dagger} |n_{-}\rangle = \sqrt{n_{-} + 1} |n_{-} + 1\rangle, \\ a_{-}^{\dagger} a_{-} |n_{-}\rangle &= n_{-} |n_{-}\rangle, \quad (n_{-} = 0, 1, 2, \dots) \end{aligned} \quad (2.2.13)$$

Thus the energy spectrum of the system is

$$E(n_{-}) = \hbar\omega_c \left[ n_{-} + \frac{1}{2} \right] \quad (2.2.14)$$



The energy eigenvalues (2.2.14) are like those of the harmonic oscillator [2]. Each is associated with a degenerate set of eigenvalues and they correspond classically to electrons orbiting perpendicularly to the applied magnetic field  $\mathbf{B}$ , but moving with a constant velocity in the direction of  $\mathbf{B}$ . They are known as Landau states and the corresponding energy levels are called Landau levels. Each Landau level is specified by a ground state of the oscillator mode. The higher Landau states are determined by applying the operator  $a^\dagger_-$  on the ground state of the system [2].

### 2.3 The Landau Problem with a Linear Potential

We now consider an extension of the ordinary Landau problem, which includes an interaction potential energy  $V(\mathbf{r})$ . This potential consists of a linear term added in the  $y$  direction.

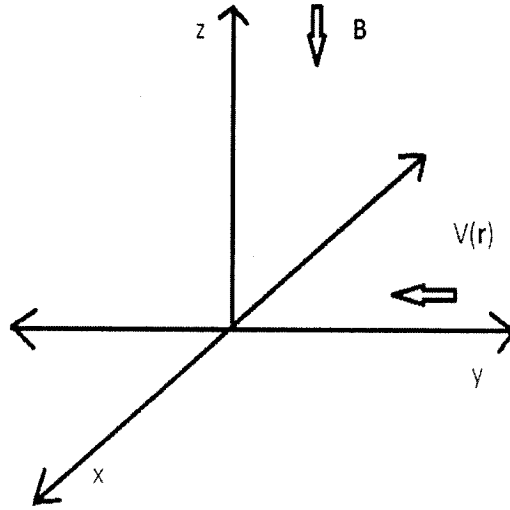


Fig.2.3: Diagram specifying the geometry of the problem for the case of when a linear potential is added

The system is then described by the Lagrangian

$$L = \frac{1}{2}m(\dot{x}^2 + \dot{y}^2) - q\mathbf{A}(\mathbf{r}) \cdot \dot{\mathbf{r}} - V(\mathbf{r}) \quad (2.3.0)$$

where

$$V(\mathbf{r}) = \gamma y \quad (2.3.1)$$

is the linear contribution to the potential energy acting along the  $y$  direction. This linear term has a strength  $\gamma$ ; this parameter is a real constant whereas  $\Lambda(\mathbf{r})$  is the vector potential. This linear potential may correspond to a constant electric field or a gravitational potential term if the plane is tilted with respect to the horizontal direction by some angle  $\alpha$ . In the latter case, one has  $\gamma = mg \cos \alpha$ .

### 2.3.1 The Landau Problem in an Infinite Plane with a Linear Potential

We first consider the Landau problem with a linear addition to the potential in the infinite plane. We employ the symmetric gauge which results in the Lagrangian:

$$L = \frac{1}{2} m (\dot{x}^2 + \dot{y}^2) - \frac{1}{2} qB (\dot{x}y - x\dot{y}) - \gamma y \quad (2.3.2)$$

The canonical momenta are

$$P_x = \frac{\partial L}{\partial \dot{x}} = m\dot{x} - \frac{1}{2} qBy, \quad P_y = \frac{\partial L}{\partial \dot{y}} = m\dot{y} + \frac{1}{2} qBx \quad (2.3.3)$$

The velocities in the  $x$  and  $y$  directions are found to be

$$\dot{x} = \frac{1}{m} \left( P_x + \frac{1}{2} qBy \right), \quad \dot{y} = \frac{1}{m} \left( P_y - \frac{1}{2} qBx \right) \quad (2.3.4)$$

The Hamiltonian

$$H = \dot{x}P_x + \dot{y}P_y - L \quad (2.3.5)$$

is found by substituting (2.3.2) and (2.3.4) into (2.3.5) to be

$$H = \frac{1}{2m} \left( P_x^2 + qB P_x y + \frac{1}{4} q^2 B^2 y^2 \right) + \frac{1}{2m} \left( P_y^2 - qB P_y x + \frac{1}{4} q^2 B^2 x^2 \right) + \gamma y \quad (2.3.6)$$

After simplification the Hamiltonian becomes

$$H = \frac{1}{2m} \left( P_x + \frac{1}{2} qB y \right)^2 + \frac{1}{2m} \left( P_y - \frac{1}{2} qB x \right)^2 + \gamma y \quad (2.3.7)$$

The algebraic treatment of the Schrödinger equation starts by making the transition from the variables  $(\hat{x}, \hat{y}, \hat{p}_x, \hat{p}_y)$  to the new ones  $(\hat{x}_c, \hat{y}_c, a_-, a_+^\dagger)$ , by means of the definitions

$$\begin{aligned} \hat{x}_c &= \frac{1}{2} \hat{x} + \frac{1}{m\omega_c} \hat{p}_y, & \hat{y}_c &= \frac{1}{2} \hat{y} - \frac{1}{m\omega_c} \hat{p}_x - \frac{\gamma}{m\omega_c}, \\ a_- &= \sqrt{\frac{m\omega_c}{2\hbar}} \left( \frac{1}{2} \hat{x} - \frac{1}{m\omega_c} \hat{p}_y \right) + \frac{i}{m\omega_c} \sqrt{\frac{m\omega_c}{2\hbar}} \left( \hat{p}_x + \frac{1}{2} m\omega_c \hat{y} + \frac{\gamma}{\omega_c} \mathbb{1} \right), \\ a_-^\dagger &= \sqrt{\frac{m\omega_c}{2\hbar}} \left( \frac{1}{2} \hat{x} - \frac{1}{m\omega_c} \hat{p}_y \right) - \frac{i}{m\omega_c} \sqrt{\frac{m\omega_c}{2\hbar}} \left( \hat{p}_x + \frac{1}{2} m\omega_c \hat{y} + \frac{\gamma}{\omega_c} \mathbb{1} \right) \end{aligned} \quad (2.3.8)$$

The inverse relations are

$$\begin{aligned} \hat{x} &= \hat{x}_c + \sqrt{\frac{\hbar}{2m\omega_c}} (a_- + a_-^\dagger), & \hat{y} &= \hat{y}_c - i \sqrt{\frac{\hbar}{2m\omega_c}} (a_- - a_-^\dagger), \\ \hat{p}_x &= -\frac{\gamma}{\omega_c} \mathbb{1} - \frac{1}{2} m\omega_c \hat{y}_c - \frac{1}{2} i m\omega_c \sqrt{\frac{\hbar}{2m\omega_c}} (a_- - a_-^\dagger), \\ \hat{p}_y &= \frac{1}{2} m\omega_c \hat{x}_c - \frac{1}{2} m\omega_c \sqrt{\frac{\hbar}{2m\omega_c}} (a_- + a_-^\dagger) \end{aligned} \quad (2.3.9)$$

We observe that  $(\hat{x}_c, \hat{y}_c)$  correspond to the coordinates of the centre of the particle's circular orbit when the magnetic force acts in the (x,y) plane. The contribution  $(-\gamma/\omega_c = -m\gamma/B)$  to

### 3.2 Discretization Method

Many numerical methods for solving different types of differential equations exist [15]. Most of these methods have reasonable accuracy and produce stable solutions for a large class of problems. However, when more realistic models of physical systems are considered, most of the methods become difficult to use and their solutions also become unstable and unusable [16]. In this case, an alternative approach to the solution of the differential equation is to transform it into a matrix equation. A lattice of discrete points is set up and the values of the solution at the lattice points are recorded. This procedure is actually a sampling of a continuous function into discrete values and leads to the formation of a linear system of coupled equations which can be written in matrix form. The solution of the original problem is then found by calculating the eigenvalues and eigenfunctions of the resulting matrix. The values of the solution at the lattice points form a vector.

#### 3.2.1 The Finite Difference Method

The finite difference method for derivatives is one of the simplest and oldest methods for solving differential equations. The principle behind this method is close to that of other numerical schemes used for solving ordinary differential equations, such as the Euler and Runge-Kutta methods. The difference is that in this method the derivatives in the differential equation are replaced by quotient approximations. The domain of integration is partitioned in space and in time and approximations of the solution are computed at the space or time points. The error in the resulting numerical solution is committed when the differential operators are replaced by the difference operators. This error is called the discretization error or truncation error. The term truncation error reflects the fact that a finite part of a Taylor series is used in the approximation.

The main concept behind the finite difference scheme is the definition of the derivative of a smooth function  $u$  at a point  $x \in \mathbb{R}$  as

$$u'(x) = \lim_{h \rightarrow 0} \frac{u(x+h) - u(x)}{h} \quad (3.2.0)$$

When  $h$  tends to 0 (without vanishing), the quotient on the right-hand side provides a ‘good’ approximation to the derivative. In other words, to get a good approximation of the solution,  $h$

should be sufficiently small. Actually, the approximation is good when the error committed in this approximation tends to zero as  $h$  tends to zero. If the function  $u$  is sufficiently smooth in the neighborhood of  $x$ , it is possible to quantify this error using a Taylor expansion.

#### 3.2.1.1 The Taylor Series and Approximation of the First Derivative

Suppose the function  $u$  is continuous and at least three times differentiable in the neighborhood of  $x$ , then for any  $h > 0$  we have the forward difference and backward difference Taylor expansions as

$$u(x+h) = u(x) + hu'(x) + \frac{h^2}{2}u''(x) + \frac{h^3}{6}u'''(\varepsilon_+) \quad (3.2.1a)$$

and

$$u(x-h) = u(x) - hu'(x) + \frac{h^2}{2}u''(x) - \frac{h^3}{6}u'''(\varepsilon_-) \quad (3.2.1b)$$

where  $\varepsilon_+ \in [x, x+h]$  and  $\varepsilon_- \in [x-h, x]$ . By subtracting these two expressions we obtain, thanks to the intermediate value theorem [17], the central difference formula for the first derivative

$$u'(x) = \frac{u(x+h) - u(x-h)}{2h} - \frac{h^2}{6}u'''(\varepsilon) \quad (3.2.2)$$

where  $\varepsilon \in [x-h, x+h]$ . The expression (3.2.2) defines a second-order consistent approximation of the first derivative.

#### 3.2.1.2 Approximation of the Second Derivative

Now, suppose  $u$  is a continuous function which is at least four times differentiable in the neighborhood of  $x$ , then for any  $h > 0$  we have the forward difference and backward difference Taylor expansions as

$$u(x+h) = u(x) + hu'(x) + \frac{h^2}{2}u''(x) + \frac{h^3}{6}u'''(x) + \frac{h^4}{24}u^{(4)}(\varepsilon_+) \quad (3.2.3a)$$

and

$$u(x-h) = u(x) - hu'(x) + \frac{h^2}{2}u''(x) - \frac{h^3}{6}u'''(x) + \frac{h^4}{24}u^{(4)}(\varepsilon_-) \quad (3.2.3b)$$

where  $\varepsilon_+ \in [x, x+h]$  and  $\varepsilon_- \in [x-h, x]$ . By adding these two expressions, we obtain the central difference formula for the second derivative

$$u''(x) = \frac{u(x+h) - 2u(x) + u(x-h)}{h^2} - \frac{h^4}{24}u^{(4)}(\varepsilon) \quad (3.2.4)$$

where  $\varepsilon \in [x-h, x+h]$ . The intermediate value theorem is again used to simplify the sum  $\frac{h^4}{24}u^{(4)}(\varepsilon_+) + \frac{h^4}{24}u^{(4)}(\varepsilon_-)$ .

### 3.2.2 The Finite Difference Formulation and the Solution of the Landau problem in the Half-plane with a Linear Potential

Having established the above theory, our focus now is to use the finite-difference method to convert the differential equation (2.3.32) into a system of equations to be solved simultaneously by transforming the problem to a matrix eigenvalue problem. If we call  $H$  the coefficient matrix of the system, then we can write the eigenvalue problem as

$$H\varphi_{E_{y_c}}(\zeta_i) = a\varphi_{E_{y_c}}(\zeta_i) \quad (3.2.5)$$

with  $a$  being the eigenvalues of matrix  $H$ .

Assuming that  $\varphi_{E_{y_c}}(\zeta)$  is a differentiable function in the closed interval  $[\alpha, \beta]$ , we introduce the equidistant grid points  $\zeta_i = \alpha + ih$ , ( $i = 1, 2, \dots, N$ ), where

$$h = \frac{\beta - \alpha}{N+1} \quad (3.2.6)$$

and  $N$  is the number of steps. At each grid point,  $\zeta_i$ , equation (2.3.32) can now be written as

$$\left( \frac{d^2}{d\zeta_i^2} - \left( \frac{1}{4}\zeta_i^2 + a \right) \right) \varphi_{E_{y_c}}(\zeta_i) = 0 \quad (3.2.7)$$

### Chapter 3. Computational Solutions of the Landau Problem

---

Now using equation (3.2.4), we can write the central-difference approximation to the second derivative as

$$\varphi_{E_{y_c}}''(\zeta) \cong \frac{\varphi_{E_{y_c}}(\zeta_{i+1}) - 2\varphi_{E_{y_c}}(\zeta_i) + \varphi_{E_{y_c}}(\zeta_{i-1}))}{h^2} \quad (3.2.8)$$

Replacing the differential operator in (3.2.7) with the central-difference approximation (3.2.8) enables us to write equation (3.2.7) as

$$\frac{\varphi_{E_{y_c}}(\zeta_{i+1}) - 2\varphi_{E_{y_c}}(\zeta_i) + \varphi_{E_{y_c}}(\zeta_{i-1}))}{h^2} - \left(\frac{1}{4}\zeta_i^2 + a\right)\varphi_{E_{y_c}}(\zeta_i) = 0 \quad (3.2.9)$$

Clearly, this equation takes different forms at the grid points  $\zeta_i = \alpha + ih$ . When applied to each point, it yields a linear system of coupled equations whose solution gives approximate values of the eigenfunctions  $\varphi_{E_{y_c}}(\zeta_i)$  of the eigenvalues  $a$ . The equation (3.2.9) must satisfy the boundary conditions of the original Schrödinger equation.

The resulting system of equations is now expressed in the tridiagonal  $N \times N$  form

$$(H - Ia)\varphi_{E_{y_c}}(\zeta_i) = 0 \quad (3.2.10)$$

where  $I$  is the unit matrix and  $H$  is the tridiagonal Hamiltonian matrix with elements

$$H_{ij} = \begin{cases} -\left(\frac{2}{h^2} + \frac{1}{4}\zeta_i^2\right) & \text{if } i = j \\ \frac{1}{h^2} & \text{if } i = j - 1 \\ \frac{1}{h^2} & \text{if } i = j + 1 \\ 0 & \text{otherwise} \end{cases} \quad (3.2.11)$$

The traditional way to solve the matrix eigenvalue problem (3.2.10) is by diagonalization. This is equivalent to successive changes of the basis vectors, each change leaving the eigenvalues unchanged while continually decreasing the values of the off-diagonal elements of matrix  $H$ . The sequence of transformations is equivalent to continually operating on the original equation with a matrix  $U$ :

$$UH(U^{-1}U)\varphi_{E_{y_c}}(\zeta_i) = aU\varphi_{E_{y_c}}(\zeta_i)$$

$$(UHU^{-})\left(U\varphi_{E_{y_c}}(\zeta_i)\right)=a\left(U\varphi_{E_{y_c}}(\zeta_i)\right) \tag{3.2.12}$$

until  $(UHU^{-})$  is diagonal:

$$(UHU^{-})=\begin{pmatrix} a_{11} & \cdots & 0 \\ \vdots & \ddots & \vdots \\ 0 & \cdots & a_{NN} \end{pmatrix} \tag{3.2.13}$$

The values of  $(UHU^{-})$  along the diagonal are the eigenvalues of the original problem.

When large matrices are considered, the diagonalization procedure of these matrices becomes very tedious and mistakes during the computations become very common. For this reason, it is very important that industrial-strength matrix subroutines from well-established scientific libraries are used. These library subroutines are usually faster than any elementary approach and are designed to minimize round off errors [18]. They also have a high chance of being successful for a broad class of problems.

In this study we use a computer program called Sci-Lab and its numerical libraries combined with the C++ programming language to solve our matrix eigenvalue problem.

We consider the different cases of a  $10 \times 10$ , an  $11 \times 11$ , a  $20 \times 20$  and  $21 \times 21$  Hamiltonian matrix and present their eigenvalues in table (3.2a) and the corresponding eigenfunctions in table (3.2b).

Now when multiplied by a factor of  $(-1)$  and up to normalization factors, (2.3.32) is the Schrödinger equation for a harmonic oscillator.

We construct  $\varphi$  to be symmetric about  $\zeta = 0$  and solve for the wave function for both positive and negative  $\zeta$  values, then use the symmetry as a check.

In general, the boundaries of the strip can be placed anywhere. For the purpose of illustrative calculations, we choose the interval  $[-4,4]$ .



10 × 10 Hamiltonian matrix	11 × 11 Hamiltonian matrix	20 × 20 Hamiltonian matrix	21 × 21 Hamiltonian matrix
- 0.4873694	- 0.4898462	- 0.4974254	- 0.4977149
- 1.435728	- 1.4488352	- 1.489285	- 1.490914
- 2.330162	- 2.3672781	- 2.486067	- 2.4913436
- 3.1677468	- 3.249186	- 3.5225772	- 3.5360097
- 3.9492235	- 4.0989795	- 4.6486551	- 4.6773844
- 4.579309	- 4.9139559	- 5.9023356	- 5.9554453
- 5.4052639	- 5.6174033	- 7.2921712	- 7.3801697
- 5.51964	- 6.4303823	- 8.8020016	- 8.9369901
- 7.3667544	- 6.5925489	- 10.402537	- 10.598508
- 7.3675993	- 8.3826405	- 12.05868	- 12.33162
	- 8.383944	- 13.732827	- 14.100635
		- 15.386405	- 15.868716
		- 16.980747	- 17.598725
		- 18.477559	- 19.253819
		- 19.838815	- 20.79777
		- 21.021675	- 22.194759
		- 22.026298	- 23.40474
		- 22.517594	- 24.425816
		- 24.003174	- 24.937522
		- 24.011855	- 26.405911
			- 26.415488

Table 3.2a: Eigenvalues of 10 × 10, 11 × 11, 20 × 20 and 21 × 21 Hamiltonian matrices in ascending order

We notice that like the results obtained in Chapter 2, those in Table (3.2a) reveal that the spectrum of eigenvalues belongs to a semi-infinite discrete set labeled as

$$a = -a_n(h), \quad n = 0,1,2, \dots, \tag{3.2.14}$$

where each of the quantities  $-a_n(h)$  is a continuous function of the step-size  $h$ .

We also notice that even though the width of the strip or equivalently the domain of integration is the same, the eigenvalues corresponding to the differently sized Hamiltonian matrices are not the same. This is so because the step-size between the lattice points is different for each matrix size. We know from Section (3.2.1) that the step-size  $h$  should be sufficiently small in order to get a good approximation of the solution. Therefore, we expect to obtain better approximations of the solution when large Hamiltonian matrices are used. In this case, our 21 × 21 Hamiltonian

matrix gives a much better approximation of the solution of the Landau problem in the half-plane with a linear potential.

For a complete solution of equation (3.2.7) and hence the Landau problem in the half-plane with a linear potential, knowledge of both the eigenvalues and corresponding eigenfunctions is required. In Table 3.2b we present the eigenfunctions corresponding to the first three eigenvalues of our most accurate Hamiltonian matrix; the  $21 \times 21$  matrix.

Eigenvalue	- 0.4977149	- 1.490914	- 2.4913436
Eigenfunctions	- 0.0057161	- 0.0208697	0.0499548
	- 0.0146353	- 0.0501177	0.1119679
	- 0.0299759	- 0.0933913	0.1873930
	- 0.0552076	- 0.1526399	0.2648767
	- 0.0933559	- 0.2233446	0.3198419
	- 0.1455791	- 0.2922300	0.3210049
	- 0.2095019	- 0.3381617	0.2455713
	- 0.2781941	- 0.3380541	0.0973958
	- 0.3407564	- 0.2767768	- 0.0839931
	- 0.3849062	- 0.1565609	- 0.2340513
	- 0.4008676	- 2.870e-15	- 0.2923111
	- 0.3849062	0.1565609	- 0.2340513
	- 0.3407564	0.2767768	- 0.0839931
	- 0.2781941	0.3380541	0.0973958
	- 0.2095019	0.3381617	0.2455713
	- 0.1455791	0.2922300	0.3210049
	- 0.0933559	0.2233446	0.3198419
	- 0.0552076	0.1526399	0.2648767
	- 0.0299759	0.0933913	0.1873930
	- 0.0146353	0.0501177	0.1119679
	- 0.0057161	0.0208697	0.0499548

Table 3.2b: The first three eigenvalues of the  $21 \times 21$  Hamiltonian matrix with their corresponding eigenvectors

Now that we have the eigenfunctions of the Hamiltonian, we can construct the full wave functions of the system. However, it should be remembered that in quantum mechanics, the wave function has no direct physical meaning, but is a theoretical construction that can be used to derive the probabilities of measurement outcomes [2]. For that reason, we do not provide any discussion regarding the construction of the wave functions. Instead we plot the eigenfunctions of the Hamiltonian corresponding to the ground state, the first excited and the second excited

Chapter 3. Computational Solutions of the Landau Problem

state energies, and then proceed to discuss applications of our solution to a two-dimensional electron gas in the next section.

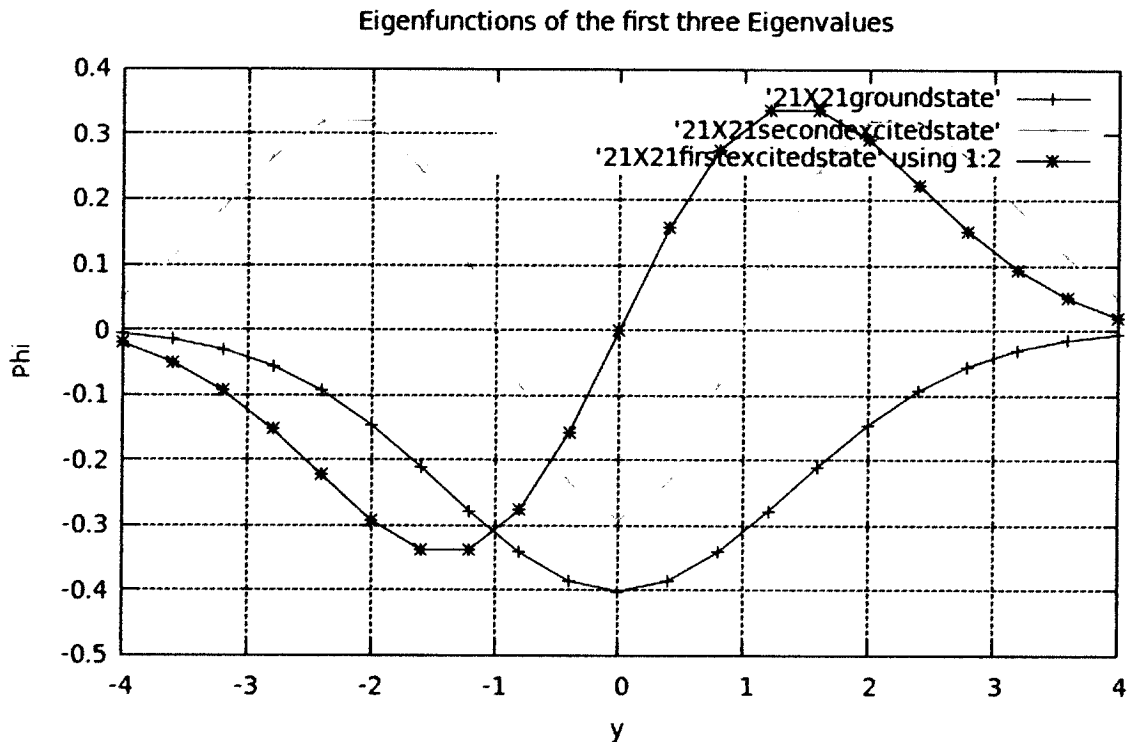


Figure 3.2: Shows plots of the ground state, first excited and second excited states of a  $21 \times 21$  Hamiltonian matrix. Observe the symmetry.

The motion of a particle is characterized by a wave function which represents a “wave packet” [2]. With reference to equation (2.3.26),  $\varphi_{E_{y_c}}(\zeta_i)$  represents the amplitude of the full wave function. Figure 3.2 depicts the form of the amplitude, it shows the dependence of the amplitude of a wave packet on the distance from its centre on the stripe  $[-4, 4]$ ; for the ground state, first excited state and the second excited state.

3.3 Landau Quantization in a Two-Dimensional Electron Gas

Finally, to complete our study of the influence of a uniform magnetic field on the dynamics of charged particles in a linear potential, we consider the time-independent problem of a two-dimensional electron system in a uniform perpendicular magnetic field. Such a system can actually be created at semiconductor heterojunctions. In this case, the classical electron orbits

can be macroscopic and there is no reason to neglect the diamagnetic contribution to the Hamiltonian.

Previously, we have worked in the symmetric gauge. However, with the algebraic solutions of Chapter 2, it does not appear possible to enforce vanishing of the wave function at two separate values of  $x$ . This is because the plane wave components in  $x$  of these wave functions derive from the eigenvalue equation for the magnetic centre coordinate  $y_c$ , which also contributes linearly to the Hamiltonian. Thus for the purpose of diagonalization of the Hamiltonian, it is convenient to adopt the Landau gauge. This idea was actually first presented by Govaerts, Hounkonnou and Mweene [5] in their study but no actual treatment was given. Here, we show that such a treatment once again leads to the parabolic cylinder functions already found in the previous section and to a finite degeneracy in the Landau levels.

Once again, we want to treat the dynamics of the system using the variational principle. We therefore start with the Lagrangian in the Landau gauge

$$L = \frac{1}{2}m(\dot{x}^2 + \dot{y}^2) - qB\dot{x}y - \gamma y \quad (3.3.1)$$

From the Lagrangian, we obtain the expressions for the canonical momenta

$$P_x = \frac{\partial L}{\partial \dot{x}} = m\dot{x} - qBy, \quad P_y = \frac{\partial L}{\partial \dot{y}} = m\dot{y} \quad (3.3.2)$$

By means of equations (3.3.2), the velocities in the  $x$  and  $y$  directions are found to be

$$\dot{x} = \frac{1}{m}(P_x + qBy), \quad \dot{y} = \frac{P_y}{m} \quad (3.3.3)$$

The Hamiltonian function, derived from

$$H = \dot{x}P_x + \dot{y}P_y - L \quad (3.3.4)$$

is obtained by substituting (3.3.1) and (3.3.3) into (3.3.4):

$$\begin{aligned} H &= \frac{P_x}{m}(P_x + qBy) + \frac{P_y^2}{m} - \frac{1}{2m}(P_x + qBy)^2 - \frac{P_y^2}{2m} + \frac{qB}{m}(P_x + qBy)y + \gamma y \\ &= \frac{P_x^2}{m} + \frac{qByP_x}{m} + \frac{P_y^2}{m} - \frac{1}{2m}(P_x^2 + 2qByP_x + q^2B^2y^2) - \frac{P_y^2}{2m} + \frac{qBP_xy}{m} + \frac{q^2B^2y^2}{m} + \gamma y \end{aligned}$$

$$= \frac{P_x^2}{2m} + \frac{P_y^2}{2m} + \frac{qBP_x y}{m} + \frac{q^2 B^2 y^2}{2m} + \gamma y = \frac{1}{2m} (P_x^2 + 2qBP_x y + q^2 B^2 y^2) + \frac{P_y^2}{2m} + \gamma y$$

Hence, the Hamiltonian can be written as

$$H = \frac{1}{2m} \left( P_x + \frac{1}{2} qBy \right)^2 + \frac{P_y^2}{2m} + \gamma y \quad (3.3.5)$$

Now we consider the diagonalization of (3.3.5) by using the wave function in configuration space rather than using Fock algebra. For the momentum and space operators we have the commutation relation

$$[\hat{x}, \hat{p}_x] = [\hat{y}, \hat{p}_y] = i\hbar \quad (3.3.6)$$

Therefore,

$$\hat{H} = \frac{1}{2m} \left( \hat{p}_x + qB\hat{y} \right)^2 + \frac{\hat{p}_y^2}{2m} + \gamma \hat{y} \quad (3.3.7)$$

The transition to quantum mechanics is made in the usual manner as

$$\hat{p}_x \rightarrow -i\hbar \frac{\partial}{\partial x}, \quad \hat{p}_y \rightarrow -i\hbar \frac{\partial}{\partial y}, \quad \Psi = \Psi(x, y)$$

Thus, we can write the Hamiltonian as

$$H = -\frac{\hbar^2}{2m} \left( \frac{\partial}{\partial x} + \frac{i}{\hbar} qBy \right)^2 - \frac{\hbar^2}{2m} \frac{\partial^2}{\partial y^2} + \gamma y \quad (3.3.8)$$

The Schrödinger equation for the system then becomes

$$-\frac{\hbar^2}{2m} \left( \frac{\partial}{\partial x} + \frac{i}{\hbar} qBy \right)^2 \Psi(x, y) - \frac{\hbar^2}{2m} \frac{\partial^2}{\partial y^2} \Psi(x, y) + \gamma y \Psi(x, y) = E \Psi(x, y) \quad (3.3.9)$$

It is evident that the wave functions of the system can be written in the separated form

$$\Psi(x, y) = e^{ikx} \varphi(y) \quad (3.3.10)$$

with

$$k = \frac{P_x}{\hbar} \quad (3.3.11)$$

Here the eigenvalues  $P_x$  take all values from  $-\infty$  to  $+\infty$ .

Resolving the terms in the Schrödinger equation (3.3.9) one at a time, we find:

$$\text{Right hand side} = E e^{ikx} \varphi(y)$$

Left hand side terms;

$$\text{Last term} := \gamma y e^{ikx} \varphi(y)$$

$$\text{Middle term} := -\frac{\hbar^2}{2m} e^{ikx} \frac{\partial^2}{\partial y^2} \varphi(y)$$

$$\begin{aligned} \text{First term} &:= -\frac{\hbar^2}{2m} \left( \frac{\partial}{\partial x} + \frac{i}{\hbar} qBy \right) \left( \varphi(y) \frac{\partial}{\partial x} e^{ikx} + \frac{i}{\hbar} qBy e^{ikx} \varphi(y) \right) \\ &= -\frac{\hbar^2}{2m} \left( \frac{\partial}{\partial x} + \frac{i}{\hbar} qBy \right) \left( ike^{ikx} \varphi(y) + \frac{i}{\hbar} qBy e^{ikx} \varphi(y) \right) \\ &= -\frac{\hbar^2}{2m} \left[ -k^2 e^{ikx} \varphi(y) - \frac{qByk}{\hbar} e^{ikx} \varphi(y) - \frac{qByk}{\hbar} e^{ikx} \varphi(y) \right. \\ &\quad \left. - \left( \frac{qByk}{\hbar} \right)^2 e^{ikx} \varphi(y) \right] = \frac{1}{2m} (\hbar^2 k^2 + 2\hbar qByk + (qBy)^2) e^{ikx} \varphi(y) \\ &= \frac{q^2 B^2}{2m} \left( y^2 + 2 \frac{y\hbar k}{qB} + \frac{\hbar^2 k^2}{q^2 B^2} \right) e^{ikx} \varphi(y) = \frac{1}{2} m \left( \frac{qB}{m} \right)^2 \left( y + \frac{\hbar k}{qB} \right)^2 e^{ikx} \varphi(y) \end{aligned}$$

After recombining all the terms, the Schrödinger equation becomes

$$\left[ -\frac{\hbar^2}{2m} \frac{d^2}{dy^2} + \frac{1}{2} m \left( \frac{qB}{m} \right)^2 \left( y + \frac{\hbar k}{qB} \right)^2 + \gamma y \right] \varphi(y) = E \varphi(y) \quad (3.3.12a)$$

This equation is exactly of harmonic oscillator form with a linear perturbation, where  $y$  is shifted by

$$y_o = \frac{\hbar k}{qB} \quad (3.3.12b)$$



### Chapter 3. Computational Solutions of the Landau Problem

---

Thus we expect a solution of the form

$$\Psi(x, y) = e^{ikx} \varphi_n(y + y_o) = e^{i\frac{qB}{\hbar}y_o x} \varphi_n(y + y_o) \quad (3.3.13a)$$

We define the cyclotron frequency of the motion of the particle as

$$\omega_0 = \frac{qB}{m} \quad (3.3.13b)$$

If we take the width of the sample in the  $x$  direction to be  $L_x$ , and assuming periodic boundary conditions, then  $y_o$  may be defined as the classical center of the electron orbit. In that case the allowed  $k$  values are

$$kL_x = 2\pi j, \quad j = 0, 1, 2, 3, \dots \quad (3.3.14)$$

This condition may also translate into a condition on the classical centre

$$y_o = \frac{2\pi j}{qBL_x} \quad (3.3.15a)$$

of the electron orbit. We must have

$$0 \leq y_o \leq L_y \quad (3.3.15b)$$

where  $L_y$  is the width of the sample in the  $y$  direction, for all the electrons to orbit inside the sample. We notice that this gives an upper bound on  $j$

$$0 \leq j \leq \frac{qB}{2\pi\hbar} L_x L_y \equiv j_{max} \quad (3.3.16)$$

Equation (3.3.14) suggests that the values of  $k$  are quantized, and equation (3.3.16) shows that the degree of degeneracy in the energy levels becomes finite if the motion is restricted to an area  $L_x L_y$ .

We now introduce the magnetic length

$$l_B = \sqrt{\frac{\hbar}{qB}} \quad (3.3.18)$$

Then the maximum number of electrons which can occupy a given Landau level is

$$j_{max} = \frac{L_x L_y}{2\pi l_B^2} \quad (3.3.19)$$

We note that (3.3.19) depends on the magnetic field. Thus the bigger the field, the more electrons can fit into a Landau level.

### Chapter 3. Computational Solutions of the Landau Problem

---

Now, we can rearrange (3.3.12a) into the form

$$\left[ -\frac{\hbar^2}{2m} \frac{d^2}{dy^2} + \frac{1}{2} m \left( \frac{qB}{m} \right)^2 \left( y^2 + 2 \frac{y\hbar k}{qB} + \frac{\hbar^2 k^2}{q^2 B^2} \right) + \gamma y \right] \varphi(y) = E \varphi(y) \quad (3.3.20a)$$

$$\left[ -\frac{\hbar^2}{2m} \frac{d^2}{dy^2} + \frac{1}{2} m \left( \frac{qB}{m} \right)^2 y^2 + \frac{qB\hbar k y}{m} + \frac{\hbar^2 k^2}{2m} + \gamma y \right] \varphi(y) = E \varphi(y) \quad (3.3.20b)$$

and finally, write the Schrödinger equation as

$$\left[ -\frac{\hbar^2}{2m} \frac{d^2}{dy^2} + \frac{1}{2} m \left( \frac{qB}{m} \right)^2 y^2 + \left( \gamma + \frac{qB\hbar k}{m} \right) y \right] \varphi(y) = \left( E - \frac{\hbar^2 k^2}{2m} \right) \varphi(y) \quad (3.3.20c)$$

If we introduce the notation,

$$\zeta = \sqrt{\frac{2m\omega_c}{\hbar}} y, \quad a = -\frac{1}{\hbar\omega_c} \left( E - \sqrt{\frac{\hbar}{2m\omega_c}} (\gamma + \hbar\omega_c) \zeta - \frac{\hbar^2 k^2}{2m} \right) \quad (3.3.21)$$

we transform the Schrödinger equation into

$$\left( \frac{d^2}{d\zeta^2} - \left( \frac{1}{4} \zeta^2 + a \right) \right) \varphi_E(\zeta) = 0 \quad (3.3.22)$$

This is in fact the same differential equation as (2.3.32), whose solutions are the parabolic cylinder functions in the  $y$  direction. Thus as far as the spectrum of eigenvalues and the eigenfunctions of the Hamiltonian are concerned, the results of Section 3.2 are still applicable. The only difference in this case will be in the value of the energy  $E$ . Nevertheless, we do not expect the values of  $E$  to vary considerably from those of Section 3.2.



## **4.0 Some uses of the Density Functional Theory in materials Science.**

---

### **4.1 Introduction**

The accurate prediction of material properties is one of the primary goals of computational condensed matter physics. For this reason current research efforts aim at developing DFT simulation software with improved accuracy for the prediction of material properties and increased ability to study very complex systems at a relatively low financial cost.

This work on the density functional theory is not related to the work presented earlier on the time-independent Landau problem.

Our aim for presenting this chapter is twofold. Firstly, we would like to demonstrate some of the capabilities of the density functional theory by performing basic electronic structure calculations on Ge, Ni, NiGe, Ni<sub>3</sub>Ge<sub>2</sub>, Ni<sub>2</sub>Ge and Ni<sub>5</sub>Ge<sub>3</sub>. Secondly, it is our hope that the study of the Ni-Ge system will help to increase awareness of research in theoretical condensed matter physics and facilitate the adoption of density functional theory calculations in future research activities in the Department of Physics at the University of Zambia.

To start, an introduction of the computer code that was used to implement the DFT calculations is given. This is followed by a series of Self-Consistent Field (SCF) calculations which are performed on the Ge, Ni and the Ni-Ge systems to obtain the total ground state energies per unit cell of the phases on the Ni-Ge phase diagram *which have been obtained experimentally*. By comparing these energies, a study on the stability of the various phases can be conducted; in turn their formation sequence can also be predicted.

## Chapter 4. Some uses of the Density Functional Theory in Materials Science

### 4.2 Plane Wave Self-Consistent Field (PWscf) Calculations

The use of plane-wave basis sets and pseudopotentials has proven to be an easy and yet fairly accurate method for performing electronic structure calculations on solids within density functional theory implemented in computer code [19].

In the present work, the calculations were performed using an open-source computer package for electronic structure calculations and simulation of molecules and solids called QUANTUM ESPRESSO [19].

The QUANTUM ESPRESSO program comprises the following core packages for calculation of electronic structure properties within density functional theory:

- PWscf (Plane-Wave Self Consistent Field) code: consists of a set of computer programs for electronic structure calculations. The PWscf code is well suited for the calculation of ground-state properties of solids and the generation of pseudopotentials.
- CP (Car-Parrinello) code: this is an *ab initio* electronic structure and molecular dynamics program using plane wave and pseudopotential implementations of density functional theory. It is mostly used for molecular simulations but also supports geometry optimizations, Born-Oppenheimer molecular dynamics, path integral molecular dynamics, response functions, excited states and calculations of some electronic properties.

All the calculations in this work were performed using the PWscf code, and thus our description of how the QUANTUM ESPRESSO program works will be focused more on the PWscf code and less on the CP code. As was outlined in Chapter 1, the Hohenberg – Kohn theorems and Kohn – Sham approach allow us to calculate the ground state energy and ground state density of an interacting electron system via the non-interacting Kohn – Sham system. The only approximation required in this approach is that for the exchange – correlation energy, which is unknown as an explicit functional of the electron density. For the QUANTUM ESPRESSO program,

#### **Chapter 4. Some uses of the Density Functional Theory in Materials Science**

the two main types of exchange-correlation functionals; local density approximation (LDA) and generalized gradient approximation (GGA) are available.

The type of exchange-correlation functional used for each calculation was read from pseudopotential files provided with the distribution. We employed the Plane Wave Self-Consistent Field method within the Generalized Gradient Approximation (GGA) of Perdew, Burke and Ernzerhof (PBE) [19] for the exchange correlation functional as implemented in the pseudopotentials provided with the QUANTUM ESPRESSO distribution.

The input files for the PWscf code were written by hand in a text editor. The input data in the input files are organized as several name-lists, followed by other fields introduced by keywords. All the input files used in this work are presented in the appendix.

Due to lack of adequate computational resources, the results presented here are only meant to illustrate the enormous potential DFT calculations have to support experimental results and their elegance and usefulness in cases where experimental techniques are not readily accessible such as in the study of low-dimensional systems.

This work was performed on a Linux system running on an Intel Pentium dual-core processor with a speed of 2 gigahertz and 2 gigabytes of memory. With this hardware architecture, only up to 50 atoms can be modeled in the simulation and the self consistent field calculations can take as long as 48 hours to run, depending on the complexity of the material being simulated, the properties being studied and the number of atoms used in the unit cell. The type of calculation being performed also influences the duration of the simulation runs.

Ideally, for complicated solid or molecular systems, parallel multi-node computer clusters with as many as 16, 24, 32 or even 48 core processors and 8 or more gigabytes of memory should be used and are recommended [19]. Calculations on these machines are much faster and more reliable as they can be optimized to the fullest potential of

#### **Chapter 4. Some uses of the Density Functional Theory in Materials Science**

the computer hardware to produce the best results possible without affecting the run-time of the simulation much.

In the next section we illustrate how an SCF (Self- Consistent Field) cycle for solving the Kohn- Sham equations proceeds.

Chapter 4. Some uses of the Density Functional Theory in Materials Science

4.2.1 Self- Consistent field cycle

The Kohn-Sham equations provide a practical way of calculating the ground state density and energy including every observable that is known to be an explicit functional of the ground state density [7]. The calculations involve solving the Schrödinger and Poisson’s equation self-consistently.

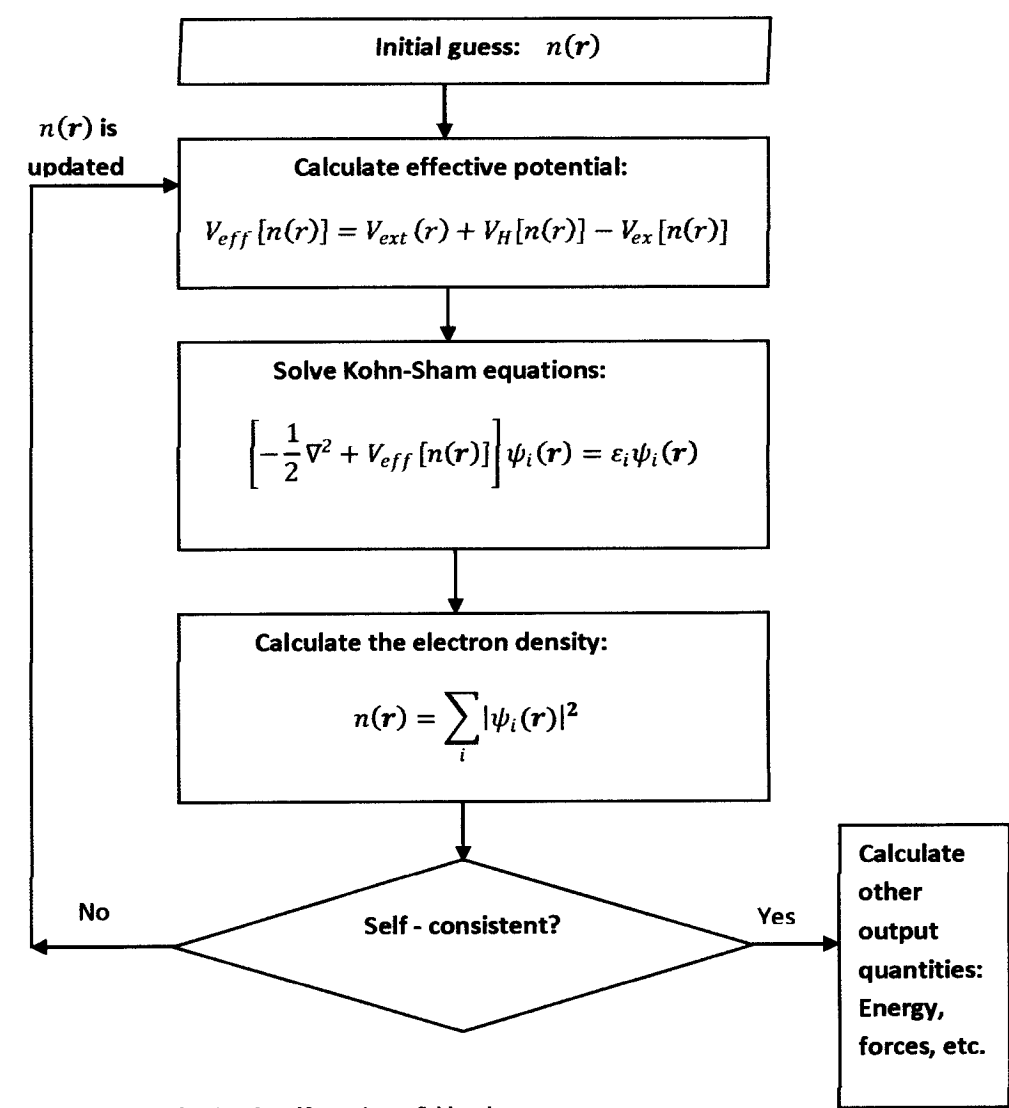


Fig. 4.2.1: Flow chart showing the self-consistent field cycle.

## **Chapter 4. Some uses of the Density Functional Theory in Materials Science**

The flow chart in Fig.4.2.1 illustrates how the process for solving the Kohn-Sham equations and Poisson's equation for the electronic charge density self-consistently proceeds.

The SCF cycle always starts with an initial guess of the electronic charge density. The charge density is used for calculating the effective potential using the Poisson equation, the solution of the Poisson equation is then used in the Kohn-Sham equations to obtain the ground state solution of the system. The solution of the Kohn-Sham equations is used to calculate the new electron density. After the density is calculated, a check is performed by the code to ensure convergence. When convergence is achieved, calculations of the observables proceed; otherwise the cycle starts all-over using the last calculation of the electronic charge density as the initial guess until convergence is achieved.

The SCF cycle has been successfully implemented in the PWscf code of the QUANTUM ESPRESSO computer package. In this work we illustrate how it works by running SCF cycles to calculate the total ground state energies of Ge, Ni, NiGe, Ni<sub>3</sub>Ge<sub>2</sub>, Ni<sub>2</sub>Ge and Ni<sub>5</sub>Ge<sub>3</sub>.

### **4.2.2 Density Functional Methods in the Study of Crystalline Materials**

Within the PWscf code, electronic and ionic structure calculations are performed after running an SCF cycle using a program called pw.x [19]. The pw.x program uses the input files written by hand in a text editor. The details of the system being studied that can be entered in the input file are, but not limited to:

- ATOMIC SPECIES;
- ATOMIC POSITIONS (In the unit cell);
- K-POINTS;
- CELL PARAMETERS;
- OCCUPATIONS.

## **Chapter 4. Some uses of the Density Functional Theory in Materials Science**

For all calculations in this study, the k-point grids were generated automatically. The automatic generation of the k-point grid follows the convention of Monkhorst and Pack [19].

### **4.3 Results**

Intrinsic crystalline Germanium has a diamond lattice structure. Its underlying space lattice is face-centered cubic and its primitive basis has two identical atoms at co-ordinates (0, 0, 0) and (1/4, 1/4, 1/4) centered at each point of the lattice. Each atom has four nearest neighbors that form a tetrahedron and the structure is bound by directional covalent bonds.

Fig. 4.3.1a and Fig. 4.3.1b show visualizations of crystalline Germanium and fcc Nickel. These were generated from the PWscf input file of the self-consistent calculation using a computer program called XCrySDen [20]. The figures present perspectives of the Germanium diamond crystal structure and face-centered cubic structure of Nickel and show how the atoms are placed in the conventional cells.

By editing the input file, any crystal structure geometry can be produced; atoms can be moved to different locations and electron-hole movements in the valence band can also be simulated [19].

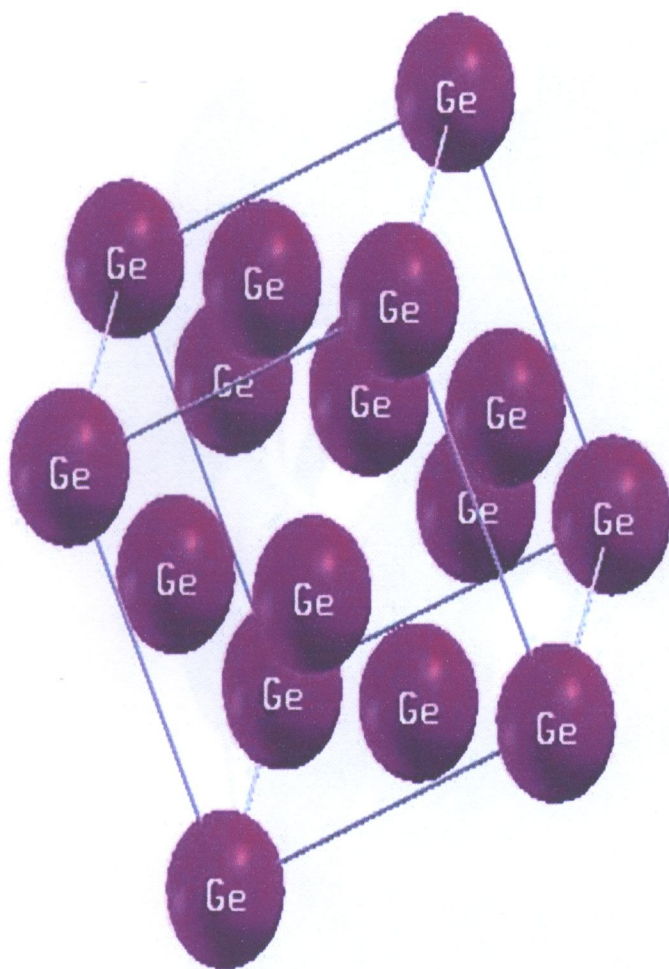


Fig 4.3.1a: Face-Centered cubic structure of Ge with a lattice parameter equal to 10.9251 Bohr



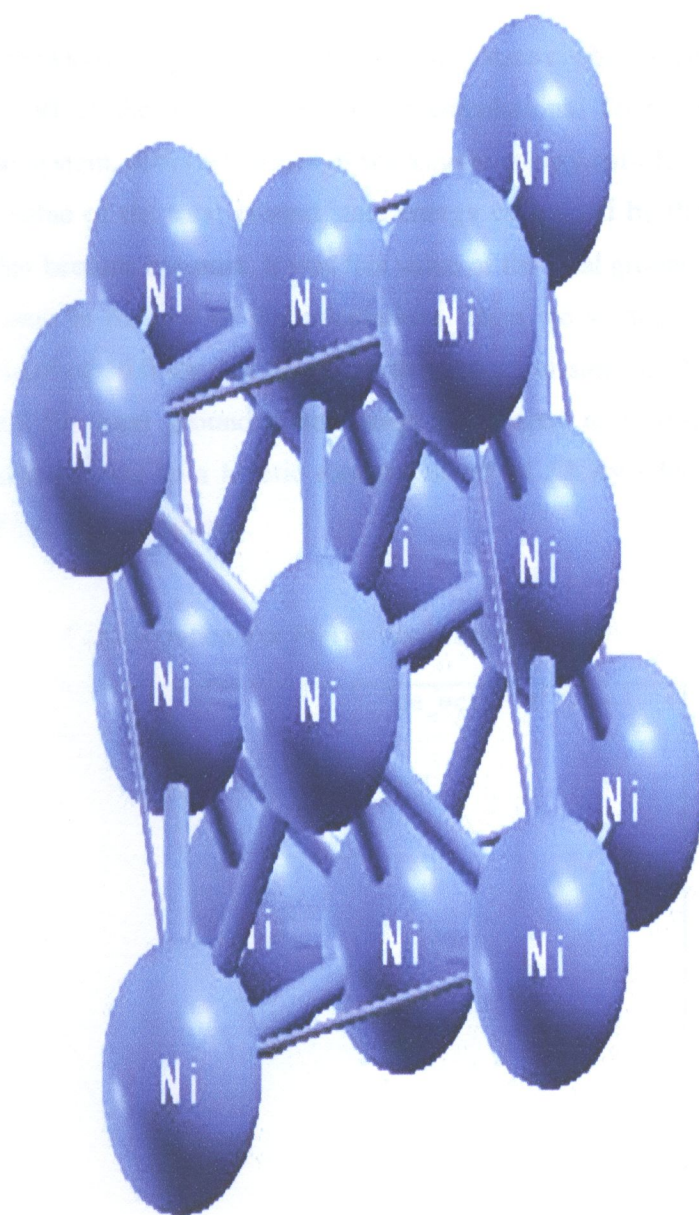


Fig 4.3.1b: Face-Centered cubic structure of Ni with a lattice parameter equal to 6.6505 Bohr

Chapter 4. Some uses of the Density Functional Theory in Materials Science

4.3.1 Convergence for Plane-Wave Energy Cut-Off

- **Germanium**

The graph below shows convergence of the total ground state energy versus the kinetic energy cut-off of the plane-waves for Ge calculations. To reach the ground state of the system, different values of the kinetic energy cut-off had to be used until the value of the total ground state energy calculated by the self consistent algorithm become constant. It was this value of the total ground state energy that was used in the rest of the calculations. Here we started with a kinetic energy cut-off of 16.0 Ry and increased this values in steps of 4.0 Ry up to 60 Ry until the total ground state energy converged to a value of -328.2124 Ry corresponding to a kinetic energy cut-off of 52 Ry which we used in the rest of the Ge calculations.

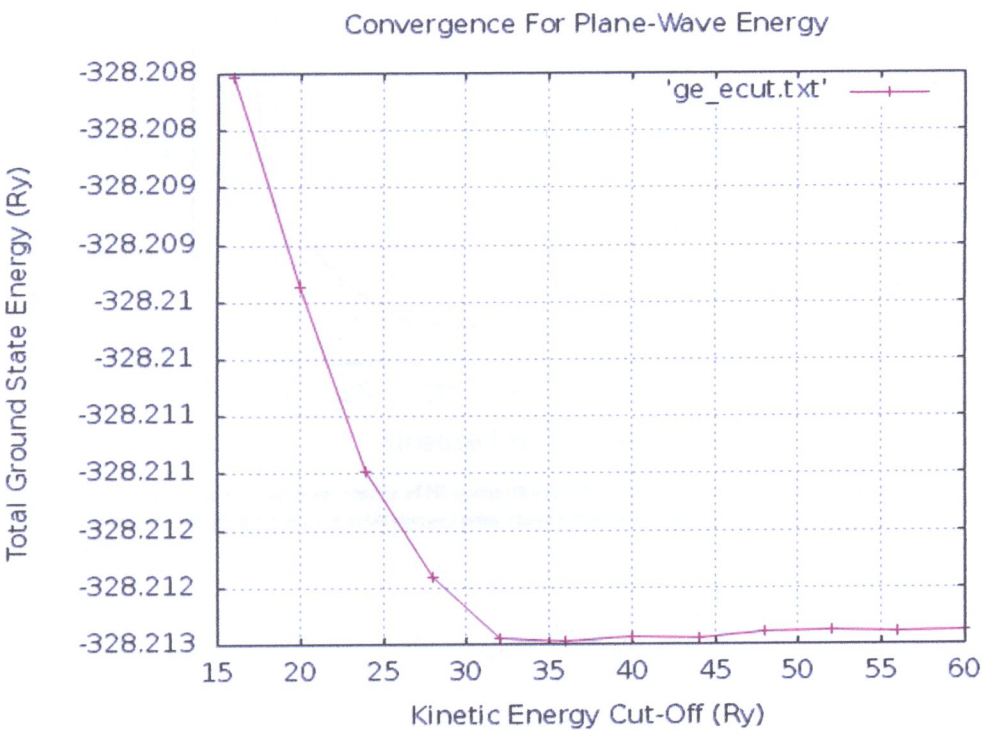


Fig 4.3.1a: Total ground state energy of Ge versus the kinetic energy cut-off. The convergence values are: -328.2124 Ry for the total ground state energy and 52 Ry for the Kinetic energy cut-off.

Chapter 4. Some uses of the Density Functional Theory in Materials Science

- **Nickel**

The graph below shows convergence of the total ground state energy versus the kinetic energy cut-off of the plane-waves in the Ni calculations. The total ground state energy converged to a value of -85.8958 Ry corresponding to a kinetic energy cut-off of 48 Ry which we used in the rest of the Ni calculations.

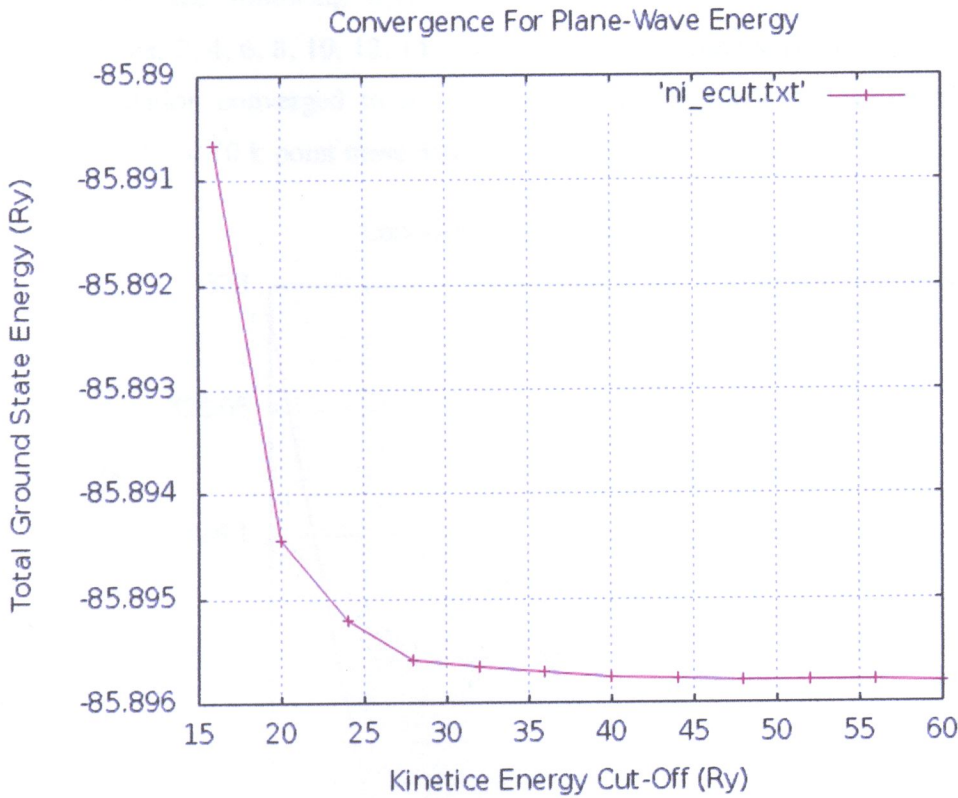


Fig 4.3.2b: Total ground state energy of Ni versus the kinetic energy cut-off. The convergence values are: -85.8958 Ry for the total ground state energy and 48 Ry for the Kinetic energy cut-off.

Chapter 4. Some uses of the Density Functional Theory in Materials Science

4.3.2 Convergence for K-Point Mesh Density

- **Germanium**

After the kinetic energy cut-off of a system is found, it is necessary to perform another convergence test for the total ground state energy. While keeping the value of kinetic energy cut-off obtained in the first test fixed (52 Ry), the number of k-points is varied in order to sample within the first Brillouin zone. With the following divisions of the three primitive reciprocal lattice vectors: 2, 4, 6, 8, 10, 12, 14, and 16, the total ground state energy for the Ge calculation converged to a value of -328.232 Ry which corresponds to a  $10 \times 10 \times 10$  k-point mesh density.

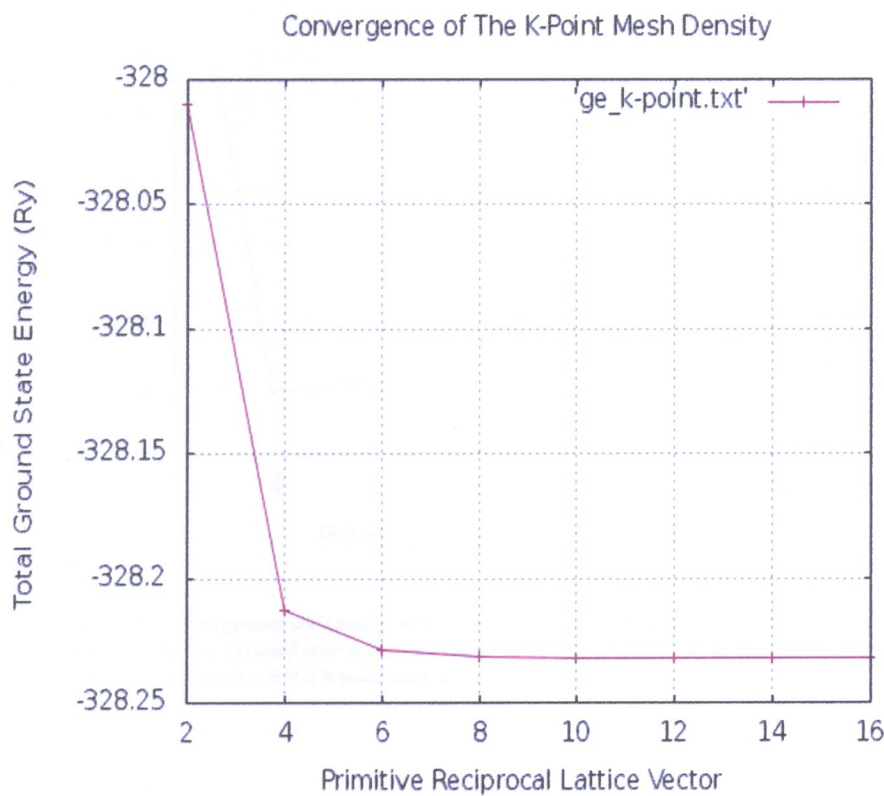


**Fig 4.3.2a:** Total ground state energy of Ge versus the primitive Reciprocal Lattice Vectors. The total ground state energy converges to a value of -328.232 Ry which corresponds to a  $10 \times 10 \times 10$  k-point mesh grid.



**Chapter 4. Some uses of the Density Functional Theory in Materials Science**

- Nickel**

Performing a similar procedure for the Ni calculation as was done for the Ge, the total ground state energy converged to a value of -85.888 Ry which corresponds to an  $8 \times 8 \times 8$  k-point mesh density.

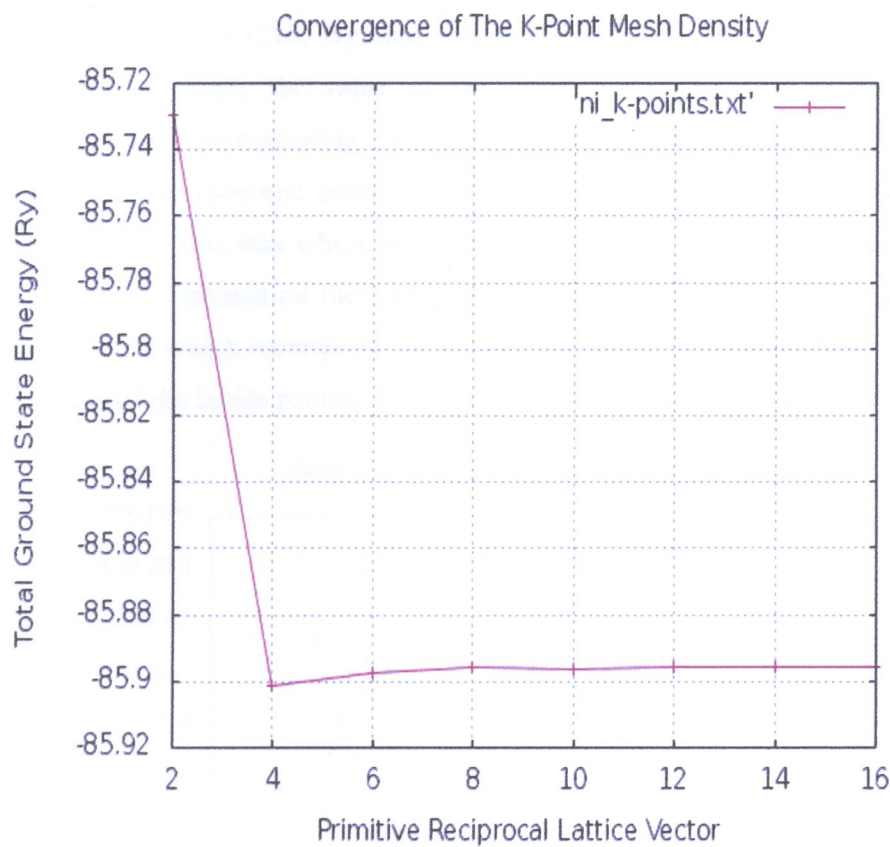


**Fig 4.3.3b: Total ground state energy of Ni versus the primitive Reciprocal Lattice Vectors. The total ground state energy converges to a value of -85.888 Ry which corresponds to an  $8 \times 8 \times 8$  k-point mesh grid.**

Chapter 4. Some uses of the Density Functional Theory in Materials Science

4.3.3 Calculation of the Lattice Parameter

- **Germanium**

The final convergence test performed involves keeping the k-point mesh density and kinetic energy cut-off values obtained in the first and second tests fixed. For the Ge calculation these were energy of 52 Ry and a k-point mesh density of  $10 \times 10 \times 10$ . By choosing a range of 3% about the approximate experimental value, the value of the lattice parameter was varied while recording the corresponding values of the total ground state energy. This procedure was executed continuously until an equilibrium lattice parameter was obtained; this was where the total ground state energy had its minimum value. In this calculation the total ground state energy had its minimum at  $-328.2346$  Ry which corresponds to a lattice parameter of 10.9251 Bohr. This is the value of the lattice parameter that is used in the calculations that followed.

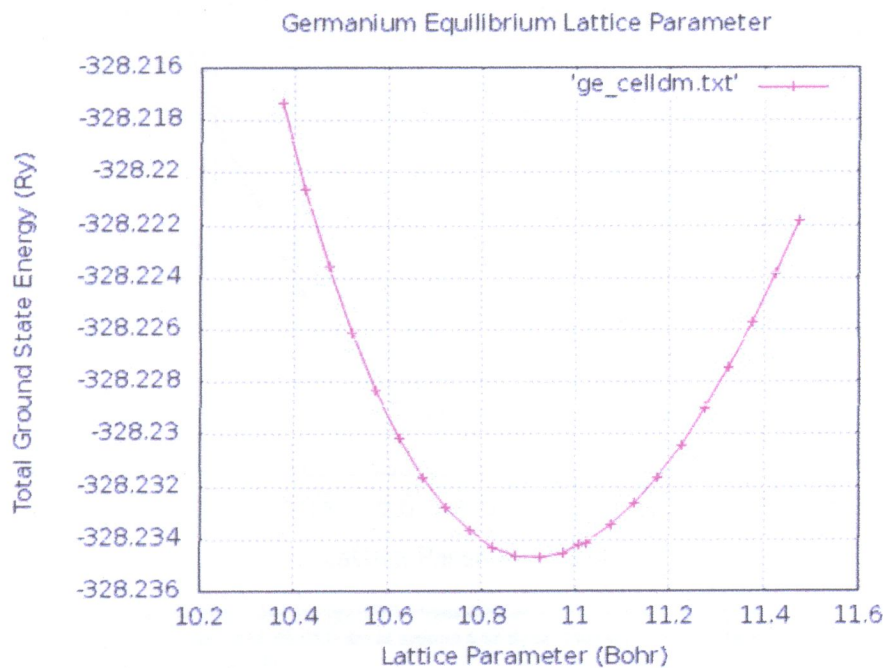
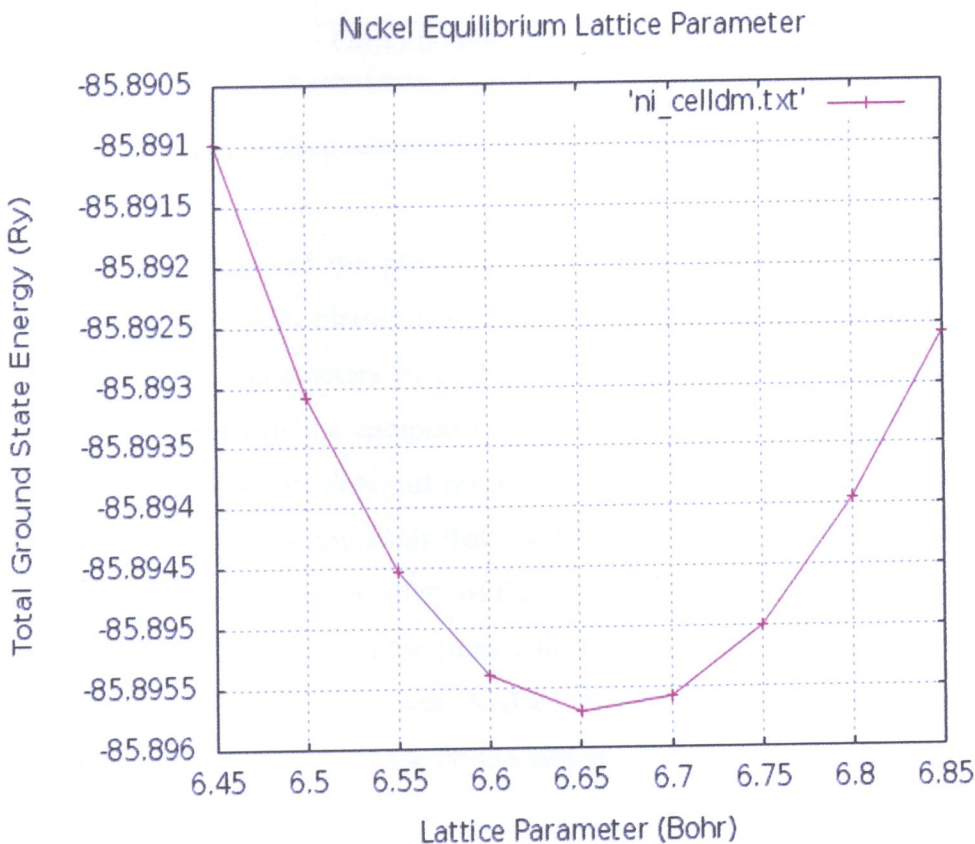


Fig 4.3.4a: Total ground state energy of Ge versus the Lattice Parameter. The system has an energy minimum of  $-328.2346$  Ry at around 10.9251 Bohr. This is the equilibrium Lattice Parameter for the Ge lattice.

Chapter 4. Some uses of the Density Functional Theory in Materials Science

- **Nickel**

A similar procedure as that which was used for the Ge calculation was also used for Ni. While keeping the k-point mesh density of  $8 \times 8 \times 8$  and a kinetic energy cut-off of 48 Ry; obtained in the first and second tests fixed, an equilibrium lattice parameter of 6.6505 Bohr was obtained. This value corresponded to a total ground state energy minimum of -85.8957 Ry and was used in all the Ni calculations that followed.



**Fig 4.3.4b:** Total ground state energy of Ni versus the Lattice Parameter. The system has an energy minimum of -85.8957 Ry at around 6.65 Bohr. This is the equilibrium Lattice Parameter for the Ni lattice.

4.4 Stability of Nickel Germanides

Phase formation of nickel germanides formed by thermal annealing has been studied widely in materials science [21, 22, 23, 24]. The table 4.0 shows experimentally obtained crystal structures and lattice parameters of some phases of the Ni-Ge system.

Phase	Crystal structure	Lattice constants (Å)		
		a	b	c
Ni <sub>2</sub> Ge	Orthorhombic	5.113	3.830	7.264
Ni <sub>5</sub> Ge <sub>3</sub>	Monoclinic	11.68	6.73	6.36
NiGe	Orthorhombic	5.389	3.438	5.82
NiGe <sub>2</sub>	Orthorhombic	10.830	5.763	5.762

Table 4.0: Crystal structures and lattice parameters of phases of the Ni-Ge system [25, 26, 27, 28].

We studied the stability of the phases of the Ni-Ge system by obtaining the total ground state energies of the phases using the PWscf code. Initially, we used the crystal structures and lattice parameters of each phase as given in table 4.0. After several attempts, it was clear that the computational power available to us was not adequate and we could not obtain meaningful results using this direct approach. We therefore adopted an approximation approach that used two model cases. These model cases made use of our results from the study of the elemental materials Ni and Ge to give us some insight into the stability of the phases in the Ni-Ge system. We picked the four phases, NiGe, Ni<sub>2</sub>Ge, Ni<sub>3</sub>Ge<sub>2</sub> and Ni<sub>5</sub>Ge<sub>3</sub>, which are commonly observed in experimental thin film studies of the Ni-Ge system. For each phase we considered the following two model cases:

1. When Ni atoms are static and Ge atoms diffuse to the Ni sites: In this case the convergence parameters for Ni obtained above in section 4.3 were used since the Ni atoms are static. A kinetic energy cut-off of 48 Ry, lattice parameter of 6.6505 Bohrs and a k-Point mesh density of  $8 \times 8 \times 8$  were used;



Chapter 4. Some uses of the Density Functional Theory in Materials Science

2. When Ge atoms are static and the Ni atoms diffuse to the Ge sites: In this case the convergence parameters for Ge obtained above in section 4.3 were used since the Ge atoms are static. A kinetic energy cut-off of 52 Ry, lattice parameter of 10.9251 Bohr and a k-Point mesh density of  $10 \times 10 \times 10$  were used.

Fig. 4.4 shows the total ground state energies that were obtained in our calculation for each of the two model cases for the NiGe, Ni<sub>2</sub>Ge and Ni<sub>3</sub>Ge<sub>2</sub> phases.

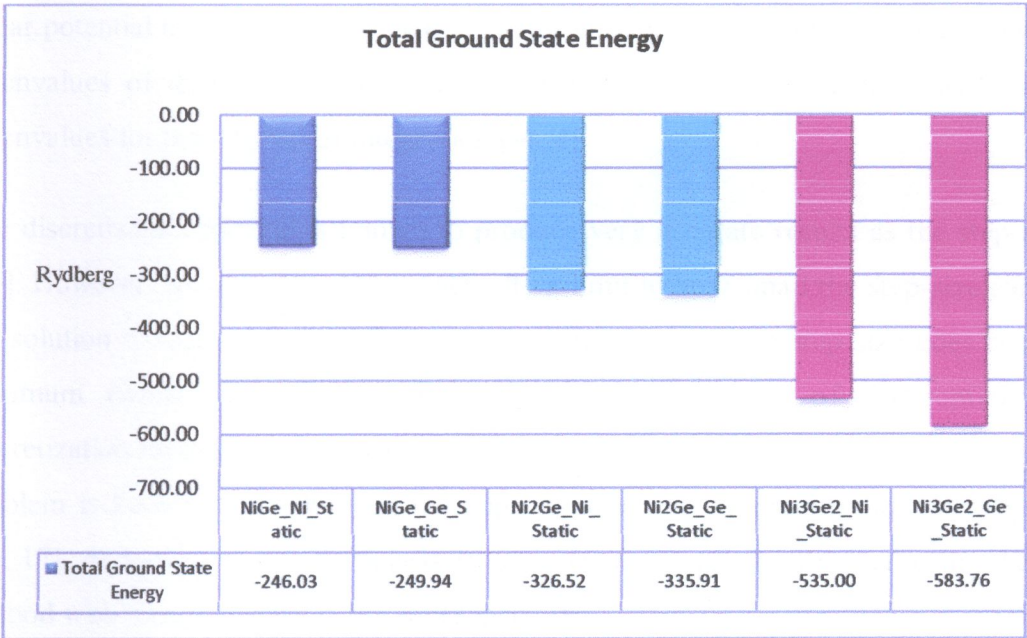


Fig 4.4: Total Ground State Energy of the NiGe, Ni<sub>2</sub>Ge, Ni<sub>3</sub>Ge<sub>2</sub> phases.

From the results we deduce that the Ni<sub>3</sub>Ge<sub>2</sub> phase is the most stable since it has the lowest ground state energy and hence is expected to form first followed by Ni<sub>2</sub>Ge while NiGe is expected to form last having the highest ground state energy. An attempt to study the Ni<sub>5</sub>Ge<sub>3</sub> phase was not successful due to lack of adequate computational resources.

---

### Discussion and Conclusion

---

#### 5.1 The Landau problem

The aim of the first part of this study was to solve the Landau problem in the half-plane with a linear potential using numerical means. The discretization method was used to obtain the energy eigenvalues of the Hamiltonian and for illustrative purposes, we presented the spectrum of eigenvalues for the interval of integration  $[-4, 4]$ .

The discretization method is known to produce very accurate results as the step-size is reduced [17]. However, we note that there is actually a limit to how small the step-size can be made. For the solution of many differential equations, as the value of the step-size goes beyond a specific minimum (while approaching zero) unique to each type of differential equation, the discretization method fails to produce the correct eigenvalues [17]. The principal source of this problem is known to result from the approximation of continuous functions by discrete ones [16, 17]. As such, it is usually necessary to compare the results obtained using the discretization method with those obtained using other methods.

Given this problem with the discretization method, it is natural to ask why another method was not chosen in the first place. The simple answer is that many numerical methods have inherent problems [15, 16, 17] such as slow convergence rates, propagation of relative and truncation errors, etc., etera. The type of problem (equations to be solved) usually influences the choice of numerical method to be used and in this study the discretization method was selected because it is fast, easy to implement in computer code and many standard library routines to be used in computer code for solving differential equations exist.

## Chapter 5. Discussion and Conclusion

Furthermore, a comparison of our results with those obtained by Mweene et al [18] using the bisection method helped to establish that Table 3.2a actually presents the correct spectrum of eigenvalues. Although the bisection method is a slowly convergent method, the fact that it is still an efficient method that can be used as a global method to get initial approximations, strengthens our faith in the results we obtained using the discretization method.

To come close to an actual situation of physical interest in the quantum Hall context, where the linear potential could be related to a constant electric field or a gravitational potential well, we considered Landau quantization in a 2-D electron gas. We considered a finite sample (Hall slab).

A derivation of the Hamiltonian in the Landau gauge revealed that the degree of degeneracy in the energy levels becomes finite if the motion of the electrons is restricted to an area and that the maximum number of electrons which can occupy a given Landau level depends on the strength of the magnetic field. The relationship between the number of electrons in a Landau level and the strength of the magnetic field is actually linear. The stronger the field, the more electrons can fit in a Landau level.

The use of the Landau gauge in this treatment once again led to the parabolic cylinder functions which were obtained as the solution when the symmetric gauge was used in an earlier chapter. For the energy spectrum, an analysis of the expression obtained after use of the Landau gauge shows that besides a term analogous to the one linear in  $\gamma y_c$ , there is another contribution whose scale is set by the Landau problem itself,  $\hbar\omega_c$ . This latter contribution remains independent of the coefficient setting the strength of the linear potential,  $\gamma$ . Thus, the only effect of introducing this extra interaction energy in the system is to slightly tilt the spectrum of the Landau levels.

As was already pointed out in [5], to assess under which experimental conditions such effects may become observable, one has to understand the functional dependence of the energy spectrum on the geometry of the slab as compared to the effects of a linear potential term which may be due to electric or gravitational interactions. Nevertheless, whatever the details of these dependences, it remains true that the factors setting the scales for these types of effects are the Landau gap,  $\hbar\omega_c$  and the potential energy,  $\gamma y_c$ .

### 5.2 The Density Functional theory and its applications in materials science

The continuous increase of computational power combined with the development of new algorithms and tools allows the application of advanced theoretical techniques in the modeling of materials of growing complexity. The density functional theory (DFT), based only on quantum mechanics and the laws of electromagnetism, has become a reliable tool for atomic scale simulations of numerous compounds and nanostructures.

The aim of the second part of this study was to introduce the density functional theory and its applications in materials science. We presented the computer program that was used to perform the calculations and how the self-consistent field algorithm works. To conclude we proved that DFT procedures provide a framework which allows comparison of measured material properties with theoretical predictions by studying crystalline materials.

In thin film reactions only some of the compounds present in the equilibrium binary phase diagram form during solid state reactions. For the Ni-Ge system only two phases are observed. The available reports agree on the second and final phase, NiGe, but disagree on the first phase. Some researchers report orthorhombic Ni<sub>2</sub>Ge [22, 23, 24] while others report monoclinic Ni<sub>5</sub>Ge<sub>3</sub> [25, 26, 27, 28, 32] or hexagonal Ni<sub>3</sub>Ge<sub>2</sub> [29] as the first phase.

Table 5.0 shows experimental results of the formation of phases in the Ni-Ge system obtained by different authors.

Chapter 5. Discussion and Conclusion

No	First phase		Second phase		Reference
	Observed phase	Typical formation temperature (°C)	Observed phase	Typical formation temperature (°C)	
1	Ni <sub>2</sub> Ge	≈ 250 160 150-300	NiGe	260-600 250 250-600	E.D. Marshal et al. [22] Y.F. Hsieh et al. [23] M.W. Wittmer et al. [24]
2	Ni <sub>3</sub> Ge <sub>2</sub>	-	NiGe	-	L.J. Lin et al. [29]
3	Ni <sub>5</sub> Ge <sub>3</sub>	- - -	NiGe	- 150 200–300	S. Gaudet et al. [25] F. Nemouchi et al. [26, 27, 30] Patterson et al. [28]
4	Ni <sub>5</sub> Ge <sub>3</sub> / Ni <sub>2</sub> Ge	250/300	NiGe	350	M. Mueller et al. [31]
5	Ni <sub>5</sub> Ge <sub>3</sub>	145	NiGe	285	J.K. Pondo [32]

Table 5.0: Observed Ni-Ge system phases and their typical formation temperatures.

In our results we reported that since the Ni<sub>3</sub>Ge<sub>2</sub> and Ni<sub>2</sub>Ge phases have relatively low total ground state energies, they are expected to be more stable than NiGe which has higher ground state energy. In relation to the formation sequence, our results indicate that Ni<sub>3</sub>Ge<sub>2</sub> and Ni<sub>2</sub>Ge should form earlier than NiGe. This is in perfect agreement with the experimental results shown in Table 5.0 above.

# Appendix: Quantum Espresso Input Files

---

## 1. Crystalline Germanium

```
&control
    calculation = 'scf',
    restart_mode = 'from_scratch',
    outdir = '/home/elias/tmp/',
    pseudo_dir = '/opt/espresso-4.2.1/pseudo/',
    prefix = 'ge',
/
&system
    ibrav = 2,
    celldm(1) = 10.9251,
    nat = 2,
    ntyp = 1,
    ecutwfc = 52.0,
/
&electrons
    conv_thr = 1.0d-8,
    mixing_beta = 0.7,
/
ATOMIC_SPECIES
    Ge 72.64 Ge.pbe-paw_kj.UPF
ATOMIC_POSITIONS
    Ge 0.000000000 0.000000000 0.000000000
    Ge 0.250000000 0.250000000 0.250000000
K_POINTS automatic
    10 10 10 0 0 0
```

## 2. Fcc Nickel

```
&control
    calculation = 'scf',
    restart_mode = 'from_scratch',
    outdir = '/home/elias/tmp/',
    pseudo_dir = '/opt/espresso-4.2.1/pseudo/',
    prefix = 'ni',
/
&system
    ibrav = 2,
    celldm(1) = 6.6505,
    nat = 1,
    ntyp = 1,
    nspin = 2,
    starting_magnetization(1) = 0.1,
    ecutwfc = 48.0,
    ecutrho = 288.0,
    occupations = 'smearing',
    smearing = 'methfessel-paxton',
    degauss = 0.02,
/
&electrons
```

```

conv_thr = 1.0d-8,
mixing_beta = 0.7,
/
ATOMIC_SPECIES
Ni 58.69 Ni.pbe-nd-rrkjus.UPF
ATOMIC_POSITIONS
Ni 0.0000000000 0.0000000000 0.0000000000
K_POINTS automatic
8 8 8 0 0 0

```

### 3. NiGe – when Ge is static while Ni diffuses to the Ge sites

```

&control
calculation = 'scf',
restart_mode = 'from_scratch',
outdir = '/home/elias/tmp/',
pseudo_dir = '/opt/espresso-4.2.1/pseudo/',
prefix = 'nige',
/
&system
ibrav = 2,
celldm(1) = 10.9251,
nat = 2,
ntyp = 2,
nspin = 2,
starting_magnetization(1) = 0.1,
ecutwfc = 52.0,
ecutrho = 288.0,
occupations = 'smearing',
smearing = 'methfessel-paxton',
degauss = 0.02,
/
&electrons
conv_thr = 1.0d-8,
mixing_beta = 0.7,
/
ATOMIC_SPECIES
Ni 58.69 Ni.pbe-nd-rrkjus.UPF
Ge 72.64 Ge.pbe-paw_kj.UPF
ATOMIC_POSITIONS
Ge 0.0000000000 0.0000000000 0.0000000000
Ni 0.2500000000 0.2500000000 0.2500000000
K_POINTS automatic
10 10 10 0 0 0

```

### 4. NiGe – when Ni is static while Ge diffuses to the Ni sites

```

&control
calculation = 'scf',
restart_mode = 'from_scratch',
outdir = '/home/elias/tmp/',
pseudo_dir = '/opt/espresso-4.2.1/pseudo/',

```

```

        prefix = 'nige',
/
&system
        ibrav = 2,
        celldm(1) = 6.6505,
        nat = 2,
        ntyp = 2,
        nspin = 2,
        starting_magnetization(1) = 0.1,
        ecutwfc = 48.0,
        ecutrho = 288.0,
        occupations = 'smearing',
        smearing = 'methfessel-paxton',
        degauss = 0.02,
/
&electrons
        conv_thr = 1.0d-8,
        mixing_beta = 0.7,
/
ATOMIC_SPECIES
Ni 58.69 Ni.pbe-nd-rrkjus.UPF
Ge 72.64 Ge.pbe-paw_kj.UPF
ATOMIC_POSITIONS
Ni 0.000000000 0.000000000 0.000000000
Ge 0.250000000 0.250000000 0.250000000
K_POINTS automatic
8 8 8 0 0 0

```

## 5. Ni<sub>2</sub>Ge - when Ge is static while Ni diffuses to the Ge sites

```

&control
        calculation = 'scf',
        restart_mode = 'from_scratch',
        outdir = '/home/elias/tmp/',
        pseudo_dir = '/opt/espresso-4.2.1/pseudo/',
        prefix = 'nige',
/
&system
        ibrav = 2,
        celldm(1) = 10.9251,
        nat = 3,
        ntyp = 2,
        nspin = 2,
        starting_magnetization(1) = 0.1,
        ecutwfc = 52.0,
        ecutrho = 288.0,
        occupations = 'smearing',
        smearing = 'methfessel-paxton',
        degauss = 0.02,
/
&electrons
        conv_thr = 1.0d-8,
        mixing_beta = 0.7,
/
ATOMIC_SPECIES

```



```

Ni 58.69 Ni.pbe-nd-rrkjus.UPF
Ge 72.64 Ge.pbe-paw_kj.UPF
ATOMIC_POSITIONS
Ge 0.000000001 0.000000001 0.000000001
Ni 0.250000000 0.250000000 0.250000000
Ni -0.250000000 -0.250000000 -0.250000000
K_POINTS automatic
10 10 10 0 0 0

```

## 6. Ni<sub>2</sub>Ge - when Ni is static while Ge diffuses to the Ni sites

```

&control
    calculation = 'scf',
    restart_mode = 'from_scratch',
    outdir = '/home/elias/tmp/',
    pseudo_dir = '/opt/espresso-4.2.1/pseudo/',
    prefix = 'nige',
/
&system
    ibrav = 2,
    celldm(1) = 6.6505,
    nat = 3,
    ntyp = 2,
    nspin = 2,
    starting_magnetization(1) = 0.1,
    ecutwfc = 48.0,
    ecutrho = 288.0,
    occupations = 'smearing',
    smearing = 'methfessel-paxton',
    degauss = 0.02,
/
&electrons
    conv_thr = 1.0d-8,
    mixing_beta = 0.7,
/
ATOMIC_SPECIES
Ni 58.69 Ni.pbe-nd-rrkjus.UPF
Ge 72.64 Ge.pbe-paw_kj.UPF
ATOMIC_POSITIONS
Ni 0.000000001 0.000000001 0.000000001
Ni -0.500000001 -0.500000001 -0.500000001
Ge 0.250000000 0.250000000 0.250000000
K_POINTS automatic
8 8 8 0 0 0

```

## 7. Ni<sub>3</sub>Ge<sub>2</sub> - when Ge is static while Ni diffuses to the Ge sites

```

&control
    calculation = 'scf',
    restart_mode = 'from_scratch',
    outdir = '/home/elias/tmp/',
    pseudo_dir = '/opt/espresso-4.2.1/pseudo/',
    prefix = 'nige',
/

```

```

&system
        ibrav = 2,
        celldm(1) = 10.9251,
        nat = 5,
        ntyp = 2,
        nspin = 2,
        starting_magnetization(1) = 0.1,
        ecutwfc = 52.0,
        ecutrho = 288.0,
        occupations = 'smearing',
        smearing = 'methfessel-paxton',
        degauss = 0.02,
/
&electrons
        conv_thr = 1.0d-8,
        mixing_beta = 0.7,
        diagonalization = 'cg' ,
/
ATOMIC_SPECIES
Ni 58.69 Ni.pbe-nd-rrkjus.UPF
Ge 72.64 Ge.pbe-paw_kj.UPF
ATOMIC_POSITIONS
Ge 0.000000000 0.000000000 0.000000000
Ge 0.250000000 0.250000000 0.250000000
Ni 0.500000001 0.500000001 0.707000001
Ni 0.707000001 0.707000001 0.500000001
Ni -0.500000001 -0.500000001 -0.707000001
K_POINTS automatic
10 10 10 0 0 0

```

## 8. $\text{Ni}_3\text{Ge}_2$ - when Ni is static while Ge diffuses to the Ni sites

```

&control
        calculation = 'scf',
        restart_mode = 'from_scratch',
        outdir = '/home/elias/tmp/',
        pseudo_dir = '/opt/espresso-4.2.1/pseudo/',
        prefix = 'nige',
/
&system
        ibrav = 2,
        celldm(1) = 6.6505,
        nat = 5,
        ntyp = 2,
        nspin = 2,
        starting_magnetization(1) = 0.1,
        ecutwfc = 48.0,
        ecutrho = 288.0,
        occupations = 'smearing',
        smearing = 'methfessel-paxton',
        degauss = 0.02,
/
&electrons
        conv_thr = 1.0d-8,
        mixing_beta = 0.7,

```

```

                                diagonalization = 'cg' ,
/
ATOMIC_SPECIES
  Ni    58.69  Ni.pbe-nd-rrkjus.UPF
  Ge    72.64  Ge.pbe-paw_kj.UPF
ATOMIC_POSITIONS
  Ni      0.000000001    0.000000001    0.000000001
  Ni      0.500000001    0.500000001    0.707000001
  Ni      0.707000001    0.707000001    0.500000001
  Ge     -0.500000000   -0.500000000   -0.500000000
  Ge      0.250000000    0.250000000    0.250000000
K_POINTS automatic
  8 8 8  0 0 0

```

## 9. Ni<sub>5</sub>Ge<sub>3</sub>- when Ge is static while Ni diffuses to the Ge sites

```

&control
    calculation = 'scf',
    restart_mode = 'from_scratch',
    outdir = '/home/elias/tmp/',
    pseudo_dir = '/opt/espresso-4.2.1/pseudo/',
    prefix = 'nige',
/
&system
    ibrav = 2,
    celldm(1) = 10.9251,
    nat = 8,
    ntyp = 2,
    nspin = 2,
    starting_magnetization(1) = 0.1,
    ecutwfc = 52.0,
    ecutrho = 288.0,
    occupations = 'smearing',
    smearing = 'methfessel-paxton',
    degauss = 0.02,
/
&electrons
    conv_thr = 1.0d-8,
    mixing_beta = 0.7,
/
ATOMIC_SPECIES
  Ni    58.69  Ni.pbe-nd-rrkjus.UPF
  Ge    72.64  Ge.pbe-paw_kj.UPF
ATOMIC_POSITIONS
  Ge      0.000000001    0.000000001    0.000000001
  Ge     -0.000000001   -0.000000001    0.000000001
  Ge      0.000000001   -0.000000001   -0.000000001
  Ni      0.250000000    0.250000000    0.250000000
  Ni     -0.250000000   -0.250000000    0.250000000
  Ni      0.250000000   -0.250000000   -0.250000000
  Ni     -0.250000000    0.250000000   -0.250000000
  Ni     -0.250000000   -0.250000000   -0.250000000
K_POINTS automatic
  10 10 10  0 0 0

```

## 10. Ni<sub>5</sub>Ge<sub>3</sub> - when Ni is static while Ge diffuses to the Ni sites

```

&control
    calculation = 'scf',
    restart_mode = 'from_scratch',
    outdir = '/home/elias/tmp/',
    pseudo_dir = '/opt/espresso-4.2.1/pseudo/',
    prefix = 'nige',
/
&system
    ibrav = 2,
    celldm(1) = 6.6505,
    nat = 8,
    ntyp = 2,
    nspin = 2,
    starting_magnetization(1) = 0.1,
    ecutwfc = 48.0,
    ecutrho = 288.0,
    occupations = 'smearing',
    smearing = 'methfessel-paxton',
    degauss = 0.02,
/
&electrons
    conv_thr = 1.0d-8,
    mixing_beta = 0.7,
    diagonalization = 'cg' ,
/
ATOMIC_SPECIES
  Ni 58.69 Ni.pbe-nd-rrkjus.UPF
  Ge 72.64 Ge.pbe-paw_kj.UPF
ATOMIC_POSITIONS
  Ni 0.000000001 0.000000001 0.000000001
  Ni 0.500000001 0.500000001 0.707000001
  Ni 0.707000001 0.707000001 0.500000001
  Ni -0.500000001 -0.500000001 -0.707000001
  Ni -0.707000001 -0.707000001 -0.500000001
  Ge -0.500000000 -0.500000000 -0.500000000
  Ge 0.250000000 0.250000000 0.250000000
  Ge -0.250000000 -0.250000000 -0.250000000
K_POINTS automatic
  8 8 8 0 0 0

```

## References

- [1] P. Lorrain and D. R. Corson, 1988 “Electromagnetic Fields and Wave” 3<sup>rd</sup> Ed. W.H. Freeman and Company, New York.
- [2] W. Greiner, 1994 “Quantum Mechanics, An Introduction” 3<sup>rd</sup> Ed. Springer.
- [3] D. Brodie, 2001 “Further Advanced Physics”, John Murray Publishers Ltd.
- [4] L. D. Landau and E. M. Lifshitz, 1965 “Quantum Mechanics, Non-relativistic theory” 2<sup>nd</sup> Ed. Pergmon Press.
- [5] J. Govaerts, M. N. Hounkonnou and H. V. Mweene, 2009 “Variations on the Planar Landau Problem: Canonical Transformations, a purely linear potential and the half-plane”, J. Phys. A: Math. Theor. 42 485209.
- [6] W. Siegel, 2005 “Fields”, arXiv: hep-th/9912205v3.
- [7] W. Kohn and L. S. Sham, 1964 “Quantum Density Oscillations in an Inhomogeneous Electron Gas”, Phys. Rev. 137, A1687.
- [8] P. Hohenberg and W. Kohn, 1964 “Inhomogeneous Electron Gas”, Phys. Rev 136 B864.
- [9] J. M. Thijssen, 2003 “Computational Physics”, Cambridge University Press.
- [10] For a discussion and references see J. R. Nicholas and M. R. Andrew, 1998 “Designed Nonlocal Pseudopotential For Enhanced Transferability”, Phys. Rev B 59. 12471.
- [11] For a discussion and references, see I. Grinberg *et al.* Phys. Rev B 69. 144118.
- [12] R. O. Jones, 2006 “Introduction to Density Functional Theory and Exchange- Correlation Energy Functionals”, NIC Series Vol. 31 pp 45-70.
- [13] W. A. Harrison, 2000 “Applied Quantum Mechanics”, World Scientific Publishing.
- [14] M. Abramowitz and I. A. Stegun, 1972, “Handbook of Mathematical Functions”, New York: Dover.
- [15] R. H. Landau and M. J. Páez, 2004 “Computational Physics”, Wiley-VCH.
- [16] P. L. DeVries, 1994 “A First Course in Computational Physics”, John Wiley and Sons INC.
- [17] R. L. Burden and J. D. Faires, 2005 “Numerical Analysis”, 8th Ed. Thomson Books/Cole.
- [18] H.V. Mweene, 2010, Unpublished notes on the solutions of the Landau problem.

- [19] P. Giannozzi et al., J. Phys.: Condens. Matter 21, 395502 \_2009\_ <http://www.quantum-espresso.org/>.
- [20] A. Kokalj, Comp. Mater. Sci., 2003, Vol. 28, p. 155. Code available from <http://www.xcrysden.org/>.
- [21] R.M. Walser and R.W. Bené, 1976 “First phase nucleation in silicon-transition-metal planar interfaces”, Appl. Phys. Lett., 28 624-625.
- [22] E. D. Marshall, C. S. Wu, C. S. Pai, D. M. Scott and S. S. Lau, 1985 “Metal-Germanium Contacts and Germanide Formation”, Mater. Res. Soc. Symp. Proc., 47 161-166.
- [23] Y.F. Hsieh, L.J. Chen, E.D. Marshall, S.S. Lau and N. Kawasaki, 1988 “Partial epitaxial growth of  $\text{Ni}_2\text{Ge}$  and  $\text{NiGe}$  on  $\text{Ge}(111)$ ”, Thin Solid films, 162 287-294.
- [24] M.W. Wittmer, M.-A. Nicolet and J.W. Mayer, 1977 “The First Phase to Nucleate in Planar Transition Metal-Germanium Interfaces”, Thin Solid Films, 42 51-59.
- [25] H. Takizam, K. Uheda and T. Endo, 200 “ $\text{NiGe}_2$ : a new intermetallic compound synthesized under high-pressure”, J. Alloys Comd., 305 306.
- [26] P. Villars and L. D. Chen, E.D. Marshall, S.S. Lau and N. Kawasaki, 1988 “Partial epitaxial growth of  $\text{Ni}_2\text{Ge}$  and  $\text{NiGe}$  on  $\text{Ge}(111)$ ”, Thin Solid films, 162 287-294.
- [27] F.R Deboer, R. Boom, W.C. Mattens, A.R. Miedema and A.K. Niessen (editors), 1998 “Cohesion in Metals: Transition Metal Alloys”, North Holland, Amsterdam.
- [28] T.B. Massalski, 1986 “Binary Alloy Phase Diagrams”, American Society for Metals, Metal Park, Ohio.
- [29] S. Gaudet, C. Detavernier, C. Lavoie, and P. Desjardins, 2006 “Reaction of thin Ni films with Ge: Phase formation and texture”, J.Appl. Phys., 100 034306
- [30] F. Nemouchi, D. Mangelinck, J.L. Lábár, M. Putero, C. Bergman and P. Gas, 2006 “A comparative study of nickel silicides and nickel germanides: Phase formation and kinetics”, Micro Electronic Engineering, 83 2101-2106.
- [31] F. Nemouchi, D. Mangelinck. C. Bergman, G. Clugnet and P. Gas, 2006 “Simultaneous growth of  $\text{Ni}_5\text{Ge}_3$  and  $\text{NiGe}$  by reaction of Ni films with Ge”, Appl. Phys. Lett., 89 131920.
- [32] J. Ken Patterson, B.J. Park, K. Ritley, H.Z. Xiao, L.H. Allen and A. Rockett, 1994 “Kinetics of Ni/a-Ge reactions”, Thin Solid films, 253 (1-2) 456-461.

- [33] L.J. Lin, K.L. Pey, W.K Choi, E.A. Fitzgerald, D.A. Antoniadis, A.J. Pitera, M.L. Lee, D.Z. Chi and C.H. Tung, 2004 "The interfacial reaction of Ni with (111)Ge, (001)Si<sub>0.75</sub>Ge<sub>0.25</sub> and (100)Si at 400 °C", Thin Solid films, 462-463 151-155.
- [34] F. Nemouchi, 2005, *Reactivite de Films nanométriques de nickel sur Substrats Silicium-Germanium* (Université Paul Cezanne Aix-Marseille III, Faculté de Sciences et Technique de Saint Jérôme.
- [35] M. Mueller, Q.T. Zhao, C. Urban, C. Sandow, D. Buca, S. Lenk, S. Estévez and S. Mantl, 2008 "Shottky-barrier height tuning of NiGe/n-Ge contacts using As and P segregation", Materials Science and Engineering B 154-155 168-171.
- [36] J. K. Pondo, 2010 "In situ Real-Time Rutherford Back Scattering Spectrometry Study of Ni/Ge Interactions", Msc. Thesis, University of Zambia.

UNITED STATES	DEPARTMENT OF	ARMY
ACCOUNTS	PROPERTY	SECTION
6281267		
No.		